J Neurophysiol 122: 2486–2503, 2019.
First published October 2, 2019; doi:10.1152/jn.00011.2019.

RESEARCH ARTICLE | *Society for the Neural Control of Movement*

A whole body characterization of individual strategies, gender differences, and common styles in overarm throwing

Antonella Maselli,[1] Aishwar Dhawan,[1] Marta Russo,[2] Benedetta Cesqui,[2] Francesco Lacquaniti,[1,2] and Andrea d'Avella[1,3]

[1]*Laboratory of Neuromotor Physiology, IRCCS Fondazione Santa Lucia, Rome, Italy;* [2]*Department of Systems Medicine and Center of Space Biomedicine, University of Rome Tor Vergata, Rome, Italy; and* [3]*Department of Biomedical and Dental Sciences and Morphofunctional Imaging, University of Messina, Messina, Italy*

Submitted 9 January 2019; accepted in final form 1 October 2019

Maselli A, Dhawan A, Russo M, Cesqui B, Lacquaniti F, d'Avella A. A whole body characterization of individual strategies, gender differences, and common styles in overarm throwing. *J Neurophysiol* 122: 2486–2503, 2019. First published October 2, 2019; doi:10.1152/jn.00011.2019.—Overarm throwing is a fundamental human skill. Since paleolithic hunter-gatherer societies, the ability of throwing played a key role in brain and body co-evolution. For decades, throwing skill acquisition has been the subject of developmental and gender studies. However, due to its complex multijoint nature, whole body throwing has found little space in quantitative studies of motor behavior. In this study we examined how overarm throwing varies within and between individuals in a sample of untrained adults. To quantitatively compare whole body kinematics across throwing actions, we introduced a new combination of spatiotemporal principal component, linear discrimination, and clustering analyses. We found that the identity and gender of a thrower can be robustly inferred by the kinematics of a single throw, reflecting the characteristic features in individual throwing strategies and providing a quantitative ground for the well-known differences between males and females in throwing behavior. We also identified four main classes of throwing strategies, stable within individuals and resembling the main stages of throwing proficiency acquisition during motor development. These results support earlier proposals linking interindividual and gender differences in throwing, with skill acquisition interrupted at different stages of the typical developmental trajectory of throwing motor behavior.

NEW & NOTEWORTHY Unconstrained throwing, because of its complexity, received little attention in quantitative motor control studies. By introducing a new approach to analyze whole body kinematics, we quantitatively characterized gender effects, interindividual differences, and common patterns in nontrained throwers. The four throwing styles identified across individuals resemble different stages in the acquisition of throwing skills during development. These results advance our understanding of complex motor skills, bridging the gap between motor control, motor development, and sport science.

dimensionality reduction; fundamental motor behavior; interindividual variability; motor development; overarm throwing

Address for reprint requests and other correspondence: A. Maselli, IRCCS Fondazione Santa Lucia, Via Ardeatina 306, 00179 Rome (e-mail: a.maselli@hsantalucia.it).

INTRODUCTION

Throwing stones, balls, or other sorts of projectiles over large distances is an exclusive skill of the Homo lineage (Darlington 1975). Other primates can throw, but only inefficiently, with poorly accurate actions that typically involve upper limb movements only (Goodall 1964; Hopkins et al. 2012). Skillful throwing actions must instead be supported by an erect bipedal stance and involve a complex sequence of movements encompassing the whole body (Pappas et al. 1985; Roach and Lieberman 2014). A pulse of kinetic energy starting in the legs progressively cumulates through pelvis, trunk, and arm movements in an increasingly rapid chain that eventually results in the explosive transfer of kinetic energy from the throwing hand into the projectile. In addition, the resulting accuracy of fast throws is strictly related to a very precise timing of finger release in relation to the arm kinematics (Hore et al. 1995). Only humans can coordinate effectively such a complex action.

In our modern times, throwing skills are typically considered in the context of ball sports. Nonetheless, overarm throwing is de facto one of the few fundamental whole body motor behaviors observed in humans (Payne and Isaacs 2012). Alongside walking, running, and jumping, overarm throwing is indeed an emergent behavior observed universally across cultures and geographical regions, even in the absence of specific training (Williams and Monsma 2006; Young 2009). A clear pattern of overarm throwing proficiency acquisition is observed independently of social and geographical backgrounds. Starting around the age of 2 yr with simple arm movements from an upright static stance, throwing proficiency naturally converges, at age 6 to 7 yr, toward a more sequenced pattern of weight shift, trunk rotation, and steps that closely resembles the strategies adopted in fast-throwing sports (Stodden et al. 2006a; Wild 1938). Although specific training plays an important role (Butterfield and Loovis 1993; Thomas et al. 1994), it is not necessary for the natural acquisition of a complex motor sequence that effectively optimizes the exploitation of human biomechanics for shooting fast and accurate projectiles (Lombardo and Deaner 2018a; Young 2009). This is taken as one compelling piece of evidence for throwing actions to stem from an inherited motor program attained throughout evolution

(Butterfield et al. 2012; Lombardo and Deaner 2018b; Young 2009).

Much evidence supports the view that throwing is an inherited motor plan, rather than a skill purely learned from training. A tight interplay between throwing proficiency and human evolution has been established in a long tradition of evolutionary studies, since Darwin pointed to the ability of hitting distant moving preys as a key factor in the natural selection (Darwin 1871). Archaeological evidence, cast within the background of evolutionary theories, indicates that the selective pressure for skilled overarm throwing played a dramatic role in shaping humans' body anatomy (Roach et al. 2013; Roach and Richmond 2015), brain structure (Calvin 1982), and cognitive abilities (Calvin 1983; Darlington 1975). It is therefore not surprising that overarm throwing is among the few fundamental behaviors currently observed in the human motor repertoire, although its selective advantage has long vanished.

Further support that throwing stems from an inherited motor plan comes from the marked gender differences observed in throwing performance (Gromeier et al. 2017; Lombardo and Deaner 2018a). A pronounced male advantage emerges very early, around the age of 3 yr, when structural differences across genders are still negligible. The gap is maintained and typically increases throughout development (Butterfield et al. 2012; Nelson et al. 1991) and is significantly larger than for other whole body motor skills, including running and jumping (Thomas and French 1985). This gender effect cannot be completely explained by societal and/or cultural factors or by physical dimorphisms (Butterfield et al. 2012; Nelson et al. 1991; Petranek and Barton 2011). This composite evidence suggests that the gender gap in throwing is rooted in the higher involvement of males in combat and hunting activities all through the evolution of the homo lineage (Lombardo and Deaner 2018a; Young 2009).

Despite the pervasive interest in throwing behavior as a window into human evolution, development, and gender differences, kinematic analysis of whole body throwing has received less attention with respect to other fundamental motor behaviors, such as reaching, grasping, or locomotion. This is partly due to naturalistic overarm throwing being a complex and extremely rapid motor action, with a large number of degrees of freedom involved (Hore 1996). To overcome this complexity, most motor studies on throwing have focused on the control of the throwing arm alone, thereby restricting gross body movements. A comprehensive set of studies, analyzing throwing while subjects were seated upright with a fixed trunk, established important insights into the crucial role of the fingers' opening timing, required to be synchronized along with a sequenced rotations of arm joints, within milliseconds, to ensure successful performances (Hore et al. 1995, 1996). Fewer studies have addressed the issue of how this fine motor control of the throwing arm and hand is coordinated with whole body movement patterns while strict constraints are still imposed on the throwing body posture (Hore and Watts, 2005, 2011). Indeed, the sensorimotor control of whole body throwing actions remains largely unexplored (Urbin 2012).

On the other hand, quantitative studies on whole body overarm throwing have been conducted in the context of sport science, with a specific focus on how elite athletes are able to optimize control strategies for maximizing performance (Hirashima et al. 2008; Southard 2002, 2009), i.e., speed and accuracy, while minimizing the risk of injury (Fleisig et al. 1995; Seroyer et al. 2010; Whiteley 2007). Consequently, the majority of studies have investigated the specificity of motor patterns adopted in fast-ball sports. For instance, a right-handed pitch in baseball begins with a wind-up phase in which the left knee moves up while the pelvis and trunk rotate rightward, followed by a stride phase in which the left leg moves forward and an arm-cocking phase in which the throwing arm moves backward. Next, the acceleration phase follows, in which the throwing arm projects the ball forward (Sachlikidis and Salter 2007). The specific sequence of steps and torsions in the wind-up, stride, and cocking phases is tuned for maximizing the storage of elastic and kinetic energy at the shoulder (Escamilla and Andrews 2009; Fleisig et al. 1995), which is then transferred onto the throwing hand, resulting in release velocities as high as 40 m/s (Stodden et al. 2005). However, outside the sports arena, such extreme velocities are deemed less essential, more so from an ecological throwing perspective. In essence, different throwing strategies resulting in moderate release velocity (at ~10 m/s) can be effective, e.g., for killing a prey at a distance of few meters (Wilson et al. 2016).

When asked to throw and hit a distant target, adults who have not being trained in throwing-relevant sports display a heterogeneous spectrum of throwing strategies. A recent study from our laboratory found a large variability in the gross whole body kinematics adopted by different throwers, including different types and combinations of stepping patterns and throwing arm trajectories (Maselli et al. 2017). However, although several studies have analyzed in depth how different throwing patterns are acquired throughout development (Payne and Isaacs 2012; Wild 1938), the question of how untrained adults perform unconstrained naturalistic throwing actions has received little attention. Thus the goal of the current work was to characterize overarm throwing from a novel perspective, drawing inspiration from recent studies on the emergence of multiple control strategies in complex motor tasks.

A motor task, at whatever complexity level, can be accomplished with a virtually infinite number of solutions in the execution space (Bernstein 1967). However, whereas simple tasks tend to be executed with a single strategy across repetitions and individuals (Flash and Hogan 1985; Morasso 1981), in complex motor tasks, multiple strategies emerge at both the intra- and interindividual levels (Bartlett et al. 2007; Cesqui et al. 2012; Ganesh et al. 2010; La Scaleia et al. 2015). The emergence of multiple execution strategies, or task solutions, has been related to optimization processes that minimize a cost function with multiple local minima or that result from different weights in the combination of distinct elementary optimality criteria (Clever et al. 2016). In a complex multijoint task such as whole body overarm throwing, it is not straightforward to assess how individual solutions might distribute in the action space, particularly when extreme levels of optimization, such as those involved in professional sports, are not required. To this end, our aim was to characterize quantitatively how the execution of throwing actions are distributed within a heterogeneous sample of untrained throwers, both at the individual and at the interindividual level. Driven by this overall objective, we addressed the following questions: Is there a continuum of strategies adopted by different individuals, or rather a limited number of discrete solutions? If so, to what extent are these solutions related to developmental aspects of throwing proficiency acquisition, and to individual and/or gender differences?

Addressing these issues requires a step-change in the way throwing actions are described, analyzed, and compared. Previous studies on overarm throwing were indeed characterized by either one of the following two main limitations. Developmental studies have typically adopted holistic approaches based on qualitative descriptions and/or categorizations of movements (e.g., steps, trunk rotations, vertical vs. horizontal movements) as observed in real time or filmed unconstrained throwing actions (Payne and Isaacs 2012; Roberton 1977; Wild 1938). Instead, quantitative descriptions have been adopted for preselected variables, e.g., release velocities (Roberton et al. 1979), temporal joint lags (Southard 2002), stride lengths, or angular displacement of specific joints (Fleisig et al. 1999; Stodden et al. 2006a, 2006b). Similarly, the majority of biomechanics and sport science studies on throwing consist in quantitatively monitoring and comparing a number of specific preselected kinematic and kinetic variables (angular velocities, joint torques, muscle activations, etc.) in relation to performance (Escamilla and Andrews 2009; Hirashima et al. 2008; Urbin et al. 2013). The preselection of critical variables constitutes the main limitation of these quantitative approaches that, by focusing on a detailed description of cues assumed to be relevant, are not suited for a comprehensive account of individual throwing strategies, and may therefore result in a risk of bias (Lees 2002; Pataky et al. 2013). In the current work, to overcome such limitations, we introduced a novel combination of dimensionality reduction and machine learning techniques that allows us to perform quantitative comparisons of the whole body kinematics of complex actions without making any prior assumption on relative relevance of specific kinematic cues. Because the main focus was the characterization of the overarm throwing motor behavior within and across individuals, we have purposely neglected the fine-tuning aspects of the actions, such as the control of ball release strategies, as well as the relationship between throwing strategy and performance.

METHODS AND MATERIAL

Three-dimensional whole body kinematics of unconstrained throwing actions were recorded from a sample of 20 untrained right-handed participants (10 female). Participants were asked to aim at one of four targets placed at a 6-m distance. Whole body kinematics were acquired through an optoelectronic system monitoring a set of retroreflective markers. Each throw was represented in terms of the three-dimensional positional trajectories of 18 markers placed on anatomical joints locations throughout the body. The data collected and analyzed were recorded in two sessions, separated in time by 22–23 mo. *Session 1* included 20 participants; the results of a different analysis of the data have been presented in a previous study (Maselli et al. 2017). The participant identifications P1–P20 adopted throughout the current article correspond to those of the previous study. In *session 2*, we re-recruited six of the participants that took part in *session 1* and asked them to perform a replica of the previous experimental session. During the period of about 2 yr between the two sessions, participants did not get involved in any throwing-related training. The complete data set included a total of 2,800 throws, of which 2,136 are from *session 1*, and the remaining 664 from *session 2*.

We conducted our main analysis on the *session 1* data set. First, we applied a spatiotemporal principal component analysis (stPCA) decomposition to obtain a compact description of the whole body kinematics of individual throws. Subsequently, this description was used to characterize individual throwing strategies, interindividual differences, and typical strategies recurrent across individuals by means of machine learning techniques. The outcomes were then considered in light of current knowledge from throwing proficiency acquisition during development and in relation to gender differences. Finally, the data set from *session 2* was examined to assess to what extent throwing motor behavior in adulthood is stable in time.

Additional information about methods and results are given in the Supplemental Material available at https://doi.org/10.6084/m9.figshare.9165287.

Participants

Twenty right-handed participants (10 female, 10 male; age 28.2 ± 6.8 yr) with normal or corrected-to-normal vision and no history of neurological conditions participated in *session 1*. Six of them (2 female, 4 male; age: 31.3 ± 9.5 yr) also participated in *session 2*. Handedness was tested with the standard Edinburgh Handedness Questionnaire that classified 18 participants as right handed [lateral index (LI): 84.8 ± 6.8] and 2 as ambidextrous (LI = 30 and 26). Participants were further asked to fill out a brief questionnaire concerning their experience with sport-related activities. Although some participants engaged in throwing sports, they did so at the amateur level, and none of them reported to be engaged in professional training. Before participating in each experimental session, all participants signed an informed consent in accordance with the Declaration of Helsinki; they received compensation for their time spent in the laboratory. The data collection was carried out in accordance with Italian laws and European Union regulations on experiments involving human participants. The protocol was approved by the Ethical Review Board of the Santa Lucia Foundation (Prot. CE/PROG.542).

Experimental Setup and Protocol

Whole body throwing kinematics were recorded with an optoelectronic system (OptiTrack; Natural Point, Inc., Corvallis, OR) consisting of 16 cameras (Flex 13) operating at 120 Hz. All positional data were reconstructed and saved through dedicated software (Motive Body 1.9, OptiTrack; Natural Point, Inc., Corvallis, OR).

In both sessions, participants performed a series of 120 overarm throws from a fixed standing position, always starting from the same posture. Participants were instructed to hit one of the four circular targets (40-cm diameter) arranged on a target board placed at 6-m distance. The targets were arranged on a rectangular board, with target centers separated by 70 cm vertically and 80 cm horizontally. Each trial started with a computer generated pure-tone sound and the instruction on which target to hit displayed on a computer monitor. The handling and communication across systems was managed through a custom-built MATLAB script integrated with OptiTrack's NatNet SDK.

Before starting the experimental session (120 trials), participants went through a standard warm-up session including shadow throws (without the ball), throws generally aimed to hit the target board, and throws aimed at single targets. Participants were explicitly instructed to perform one-handed overarm throws without any specific constraints other than starting from the same initial "A" pose (facing the targets/board and standing upright with arms along the body and hands slightly separated from the hips).

Data Collection and Preparations

Participants were fitted with a Velcro suit and a beanie cap, on which retroreflective markers (14-mm diameter) were attached. Each participant was equipped with a standard biomechanical marker set consisting of 57 retroreflective markers. Eight of these markers, located on medial anatomical joints, were used only for calibration and were removed postcalibration. The Motive software allowed for a real-time automatic reconstruction of the moving participant's skeleton and for saving data with automatically labeled markers. A customized foam ball (40 g, 90-mm diameter) was used as projectile. The ball was embedded with five asymmetrically located retroreflective markers; subsequently, a rigid body was created to track its trajectory. Information from the ball trajectory was exclusively used to determine the time of ball release. For the analysis, each throwing action was described as a collection of spatial trajectories from a subset of 18 joint markers distributed across the whole body: left and right metatarsal (foot), lateral malleolus (ankle), femur epicondyle (knee), iliac crest (pelvis), acromion (shoulder), humerus epicondyle (elbow), ulnar styloid process (wrist), second proximal phalanx (hand), seventh cervical vertebra (cv7), and anterior head. The head position was estimated as the mean of the right and left anterior head markers.

Positional data were interpolated using a cubic spline method (to fill recording gaps) and subsequently filtered using a zero-lag Butterworth filter of order 10 and low-pass frequency 15 Hz. For each trial, the throwing action kinematics were delimited from action onset (the time at which the right-hand movement was initiated) to ball release, using the same automatized event-identification procedures described in Maselli et al. (2017). About 10% of the recorded trials were discarded due to poor tracking: 2,136 of the 2,400 trials in *session 1* and 664 of the 720 trials recorded in *session 2* were included in the analysis.

All trials from all throwers were time-aligned by normalizing their duration to the average throwing movement time of 1.2 s, and the corresponding kinematics were resampled on 100 data points. Additionally, the positional data were spatially scaled so that all participants' height after scaling corresponded to the average height (171 cm), whereas the individual relative lengths of body segments were preserved.

stPCA Decomposition

To provide a compact description of whole body throwing actions, we performed a spatiotemporal principal component analysis (stPCA) decomposition, previously introduced for the description of muscle activities (Klein Breteler et al. 2007; Russo et al. 2014), joint torques (Russo et al. 2014), and kinematics of single joint markers (Maselli et al. 2017). The method consists in a standard PCA decomposition applied to a data set in which each time sample of each time-dependent variable is treated as a feature by itself. This is different from the standard representation of a movement, typically consisting in an $N_f \times N_t$ matrix in which the temporal evolution of each one of many variables (e.g., positions, joint torques, or muscle activities) is given in one of the N_f rows, as a set of N_t time samples. Instead, since each time sample is treated as a variable, a movement is described by an $N_F \times 1$ vector, with $N_F = N_f \times N_t$. In this study, because we described the whole body kinematics as a set of 18 three-dimensional spatial trajectories, each throwing action was represented by a N_F-dimensional vector (x_i), with $N_F = 5{,}400$ (18 joint markers $\times$ 3 Cartesian coordinates $\times$ 100 time samples). The whole data set including all throws from all participants could therefore be arranged into an $N_F \times N_T$ matrix, $X = [x_1, x_2, ..., x_{N_T}]$, with N_T being the number of throws in the data set. Applying standard PCA to the matrix X allows us to identify a set of vectors $\boldsymbol{p}^{ST}$ that can be linearly combined for reconstructing all the throws in X:

$$x_i = \bar{x} + \sum\nolimits_{j=1}^{N_F} c_{i,j} \boldsymbol{p}_j^{ST},$$

where $\bar{x}$ represents the mean throw, defined as the set of joint-marker trajectories averaged across all trials from all participants (shown in Supplemental Fig. S3), and $c_{i,j}$ are scalar coefficients. In turn, each $\boldsymbol{p}_j^{ST}$ can be rearranged into a set of 18 spatial trajectories that, when added to $\bar{x}$, represent a whole body movement spanning the whole duration of the throwing action (see Fig. 3 and Supplemental Fig. S4). The $\boldsymbol{p}^{ST}$ vectors can be therefore interpreted as building blocks of whole body movements that, appropriately weighted and combined, allow us to describe the whole body kinematics of all throwing actions in the data set. As in standard PCA, $\boldsymbol{p}^{ST}$ vectors are ordered according to the amount of data variation accounted for so that the first few components can typically account for a large fraction of the total variation. In this way, an extremely compact representations at a good level of accuracy can be achieved.

Identity and Gender Recognition

Linear discriminant analysis (LDA) was applied to stPCA representations of the throwing kinematics to explore whether it would be possible to recognize the identity or gender of a thrower based on approximated low-dimensional descriptions of single throwing actions. LDA is a standard supervised classification technique used to allocate new observations into one of $N_G \geq 2$ known groups (usually referred to as classes), based on previous observations for which the group assignment is known (training data set). The method consists in finding discriminant functions that divide the features space into N_G regions, by maximizing the ratio of the between-groups to the within-group variabilities in the training set (Mardia et al. 1979). We applied LDA to the 20-class problem of identity recognition, as well as to the 2-class problem of gender recognition. The Euclidian distance in the stPCA coefficients space was used as metric for the distance between two observations. LDA results are reported in terms of the misclassification errors (MEs), as resulting from a leave-one-out cross-validation procedure. The latter consists in performing the classification assignment of each single observation (the one left out) based on the training set defined by the rest of the observations, repeating the same procedure for all observations in the data set, and defining ME as the percentage of misclassified observations. LDA performances for both classification problems have been examined for the case of different stPCA dimensionalities (from 1 to 10 dimensions).

Cluster Analysis

We applied cluster analysis to the entire set of throwing actions (all trials from all participants) with the aim of exploring the existence of typical throwing styles, recurrent across individuals. Cluster analysis is a standard unsupervised machine learning method used to group a set of observations based on their reciprocal similarity. The method was applied in the five-dimensional stPCA coefficient space, using the Euclidean distance as the metric quantifying the distance between throws. We opted for the k-means clustering method, in particular using the k-means++ method for cluster center initialization (Arthur and Vassilvitskii 2007), and performed 20 replications to further minimize the possible impact of misleading local minima. Because the k-means method requires the number of clusters N_k as an input, we first determined the optimal clustering solution, namely, the optimal value of N_k in the range 1 to 10, using three different methods: the Calinski–Harabasz method (Calinski and Harabasz 1974), the Silhouette method (Rousseeuw 1987), and the Davies–Bouldin method (Davies and Bouldin 1979). Additionally, we directly tested the hypothesis that our data were actually structured into clusters. To this end, we computed the normalized Hubert statistics for the optimal number of clusters. We then compared it with the statistics obtained for the same number of clusters identified in 100 sets of the same number of random stPCA coefficients uniformly distributed between the 2.5% percentile and the 97.5% percentile of each stPCA coefficient (Theodoridis and Koutroumbas 1999).

Additional Analysis on Stepping Patterns and Throwing Arm Trajectories

Results from the cluster analysis were next inspected to characterize how the stepping patterns and the throwing arm trajectories were distributed in each cluster. For characterizing the stepping pattern in each throw, we computed the length of the right and left feet paths from action onset to ball release, indicated thereafter as L_{RF} and L_{LF}. To analyzes the distribution of arm trajectories, we first considered the kinematics of the throwing arm joint markers (right elbow, right wrist, and right hand) in a body-centered reference frame with the origin fixed at the right shoulder location, the *x*-*z* plane aligned with the frontal plane (the *x*-axis directed from the left to the right shoulder and the *z*-axis orthogonal to it and directed upward), and the *y*-*z* plane aligned with the sagittal plane (the *y*-axis pointing outwards in the direction of throw). Furthermore, we characterized each hand trajectory with two spatial parameters quantifying the extent of lateral and anterior excursions during the rising phase. More specifically, we considered the kinematics of the hand from onset to the time at which the hand rose above the right shoulder: $t_R = \min[t; z(t) > 0]$. The lateral excursion was next defined as the *x* value corresponding to the maximum or minimum displacement from the initial position, selecting the value with the larger absolute value. An analogous definition was applied to the *y*-coordinate to define the anterior excursion. These two features were introduced for differentiating among alternative modalities of throwing behavior that have been observed and categorized in developmental studies (Roberton 1977; Roberton et al. 1979): the throwing arm trajectories opening outward vs. moving inward, and/or moving backward vs. projecting forward in the direction of throws, during the initial rising phase.

RESULTS

Intra- and Interindividual Differences Are Reflected in Throwing Kinematics

When asked to throw at 6-m distant targets, participants exhibited a heterogeneous spectrum of individual throwing strategies. For this study we define individual strategies as the set of joint-marker trajectories (from action onset to ball release) averaged across all throws from each individual, independently of the aimed target and the associated performance. Figure 1 shows all the individual strategies observed in *session 1*. Clear interindividual differences can be appreciated in gross movement components as stepping patterns, arms trajectories, and their combinations. Interindividual differences are also clear at the level of the intraindividual variability, shown for two representative participants (P1 and P4) in Fig. 2*A*. Whereas P4 appears stable across trials, with variability mainly present in the throwing arm kinematics, P1 exhibits large intertrial variability. A comprehensive view of the interindividual differences in the subjective variability is given in Fig. 2*B*, where the heatmap shows the normalized intraindividual variability characterizing the spatial trajectories of single joint markers, and the bar plot shows the corresponding average across all joint markers. Intraindividual variabilities are quantified in terms of spatial standard deviations ($std_{intra,j}$) averaged over time and are normalized to the interindividual standard deviations (std_{inter}).

For the majority of participants, intraindividual variability represents a small fraction of the variability across participants. This suggests that, with few exceptions (e.g., P1 and P20), individual strategies are well characterized despite the variations associated with *1*) different task conditions, i.e., throwing to different targets, and *2*) intrinsic variability in motor execution. This supports the validity of the definition of individual throwing strategy as the set of trajectories averaged across all throws for each individual. To keep trace of the level of intraindividual variability, we introduced a stability index, $S_j = 1 - [std_{intra,j}/std_{inter}]$, which quantifies to what extent an individual *j* reproduces similar kinematics across different throws executions (values are listed in Table 1).

stPCA Provides Compact Descriptions of Whole Body Throwing Actions

When applying stPCA to all the trials of the *session 1* data set, we found that the first 5, 10, and 23 $\boldsymbol{p}^{ST}$ components accounted for 75%, 90%, and 97% of the total variation, respectively (Supplemental Fig. S1). When the averaged trials of each participant, i.e., individual throwing strategies, are considered, stPCA leads to an

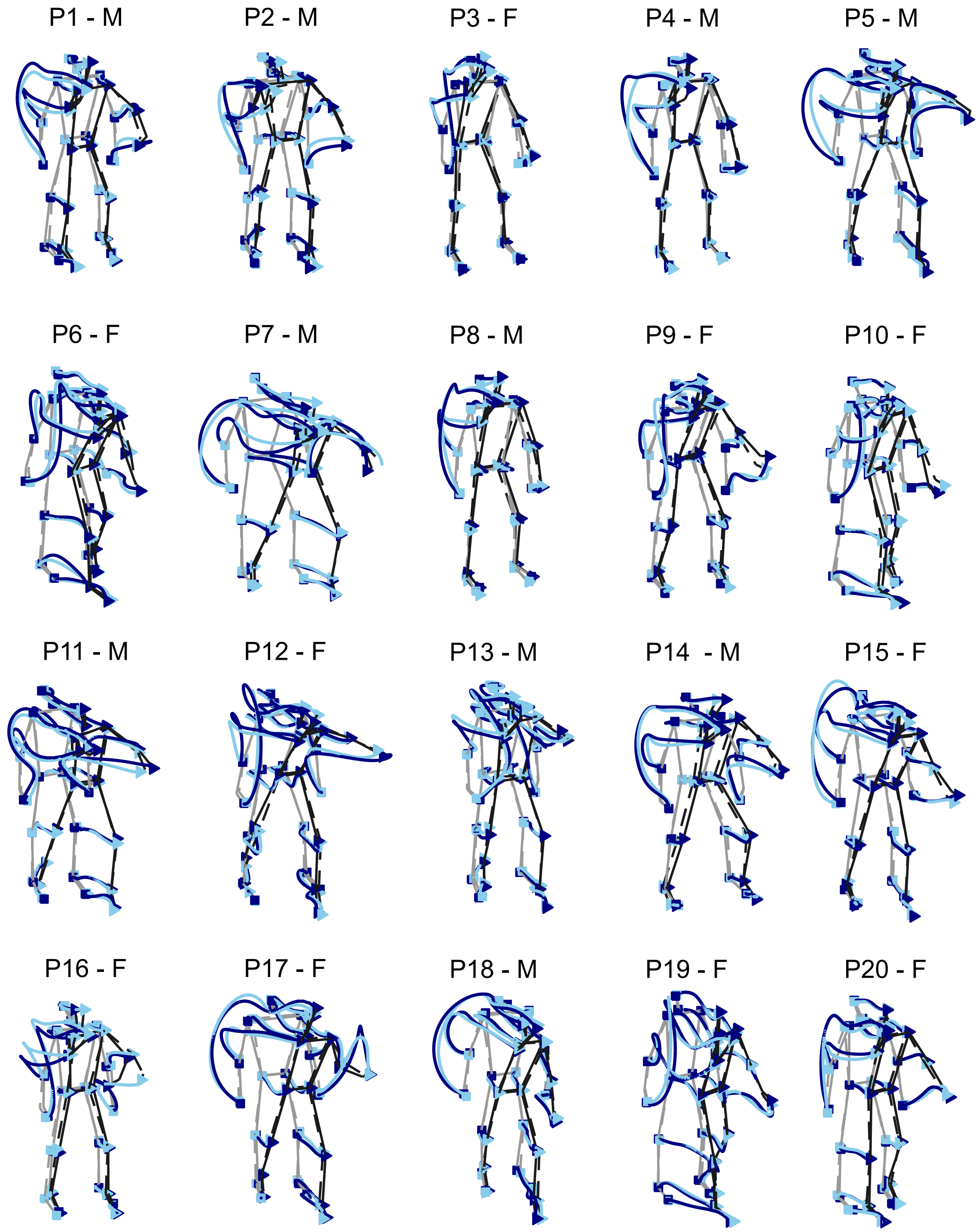

Fig. 1. Interindividual differences in throwing kinematics. Mean joint-marker trajectories (averaged over all trials performed, independently of the aimed target) are shown for all the 20 participants (P1–P20) in *session 1* (dark blue trajectories). Trajectories are displayed from the throwing action onset to ball release. Stick diagrams and corresponding joint-marker trajectories are shown from a right-frontal perspective. Posture and joint-marker positions at action onset are shown by gray solid-line stick diagrams and squares. Similarly, black solid-line stick diagrams and triangles represent the posture at ball release. Individual throwing kinematics, as approximately described in vector space defined by the first 10 spatiotemporal principal components vectors, $\boldsymbol{p}^{ST}$ (light blue trajectories), are shown along with corresponding original data. Dashed-line stick diagrams represent the $\boldsymbol{p}^{ST}$ reconstructed posture at action onset (gray) and ball release (black). The gender of each participant (F, female; M, male) is indicated above the corresponding throwing kinematics.

even higher accuracy. Figure 1 shows the comparison of the recorded individual throwing strategies with the corresponding approximated descriptions resulting from a 10-dimensional reconstruction of the kinematics. Despite the dramatic reduction in dimensionality, the approximated descriptions capture the main features of the original individual strategies. The accuracy of the description increases rapidly with the number of $\boldsymbol{p}^{ST}$ components used for the reconstruction. However, five-dimensional descriptions are already suited for capturing the main features of a throwing strategy (Supplemental Fig. S2).

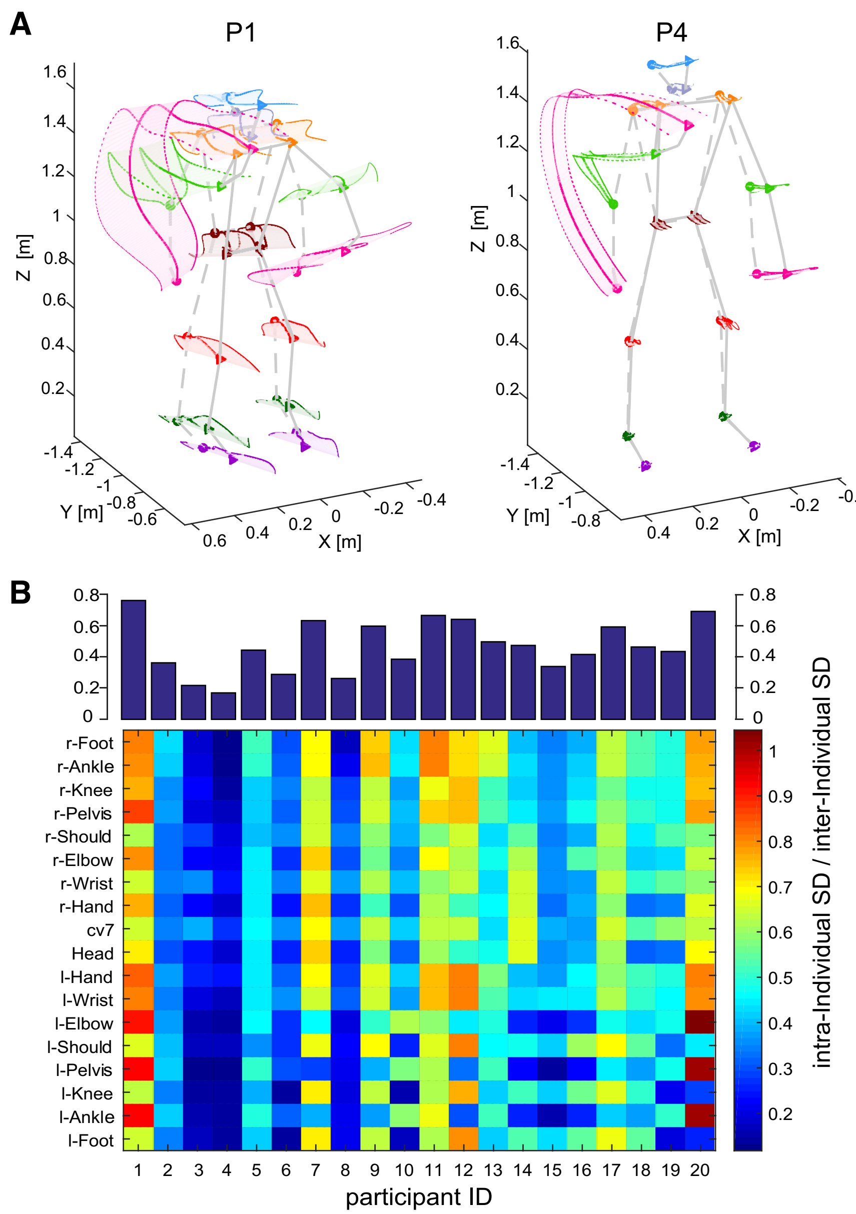

Fig. 2. Intraindividual variability. *A*: examples of intraindividual variability in throwing action for representative participants P1 and P4 (those with higher and lower variability, respectively). Stick diagrams and corresponding joint-marker trajectories are shown from a right-frontal perspective. Solid lines represent the joint-marker trajectories averaged over 104 throws from P1 and 118 throws from P4, whereas the corresponding shaded areas encompass the corresponding variability within ±1 SD. Different colors correspond to different joint markers. Posture and joint-marker positions at action onset are shown by gray dashed-line stick diagrams and circles. Similarly, gray solid-line stick diagrams and triangles represent the posture at ball release. *B*: heatmap shows the intraindividual variability ($\mathrm{std}_{\mathrm{intra}}$), normalized to the corresponding interindividual variability ($\mathrm{std}_{\mathrm{inter}}$), for each participant and all the 18 joint markers included in the analysis. Bar plot shows the corresponding normalized mean intraindividual variability (averaged across joint makers) for each participant. Variability is defined as the mean standard deviation across all trials averaged across time for each joint marker in the heatmap and further averaged across joint markers in the bar plot. cv7, Cervical vertebra 7; ID, identification; l, left; r, right; should, shoulder.

Principal components vectors. Figure 3 provides two visual representations of the whole body movement patterns associated with the first three $\boldsymbol{p}^{ST}$ vectors, offering an intuitive view of $\boldsymbol{p}^{ST}$ as building blocks of whole body movements. Figure 3, *top*, shows how each $\boldsymbol{p}^{ST}$ modifies the mean throw when added or subtracted with a unitary weight. The corresponding heatmaps (Fig. 3, *bottom*) show the spatiotemporal structure of a single $\boldsymbol{p}^{ST}$, which corresponds to the displacement from the mean throw associated to a positive unitary weighted $\boldsymbol{p}^{ST}$ contribution.

The first vector, $\boldsymbol{p}_1^{ST}$, is associated with the left foot stepping backward and the right foot forward or vice versa depending on the sign of the associated coefficient. Concomitantly, the left arm shifts backward and leftward. The second vector, $\boldsymbol{p}_2^{ST}$, is associated with a bulk motion of the whole body in the forward direction, corresponding to increments along the positive *y*-axis visible in the heatmap for all joint markers. The larger displacement at shoulders level with respect to the displacement of the pelvis corresponds instead to a trunk forward tilt. Similarly, $\boldsymbol{p}_3^{ST}$ corresponds to a bulk lateral shift, as indicated in the heatmap by the clear displacement along the negative *x*-axis (Fig. 3, *bottom*, *left* side of heatmaps) of all joint markers. Concurrently, the left arm rises and moves forward, with respect to the mean throw trajectories. Similarly to $\boldsymbol{p}_1^{ST}$, $\boldsymbol{p}_4^{ST}$ is characterized by a stepping pattern with the feet moving in opposite directions (Supplemental Fig. S4).

Higher order $\boldsymbol{p}^{ST}$ components exhibit a complex and unsystematic spatiotemporal structure, always involving the throwing arm besides other $\boldsymbol{p}^{ST}$-specific body segments (Supplemental Fig. S4). This indicates that, differently from the first four $\boldsymbol{p}^{ST}$ characterized by coordinated whole body movement patterns, higher order components play a key role in fine-tuning the limb trajectories, and thus allow reconstruction of the fine details of single throws.

Table 1. *Relevant demographic information, throw duration, and results of analysis for participants in session 1*

Participant ID	Height, m	Throw Duration, s	Gender	Stability Index	Identity Recognition Rate, %		Style Assigned			
					5D	10D	NS	RS	LS	DS
				Cluster S1: no-step						
P1	1.84	1.61 ± 0.29	M	0.24	26	89	**33**	23	28	16
P3	1.55	1.04 ± 0.23	F	0.78	93	100	**100**			
P4	1.82	0.81 ± 0.07	M	0.83	99	100	**100**			
P8	1.70	0.92 ± 0.13	M	0.74	68	95	**100**			
P9	1.59	1.13 ± 0.22	F	0.40	80	99	**89**	5	6	
P16	1.62	1.05 ± 0.15	F	0.58	70	100	**72**		28	
P20	1.63	1.27 ± 0.36	F	0.31	15	96	**54**	44	2	
				Cluster S2: right-step						
P6	1.80	1.41 ± 0.12	F	0.71	96	100		**100**		
P10	1.51	1.02 ± 0.21	F	0.61	86	99	14	**86**		
P19	1.62	1.70 ± 0.36	F	0.56	94	97		**100**		
				Cluster S3: left-step						
P5	1.90	1.12 ± 0.10	M	0.56	92	99	2		**86**	12
P7	1.80	1.00 ± 0.32	M	0.37	93	97	3		**97**	
P12	1.53	1.27 ± 0.15	F	0.36	88	99	12		**86**	2
P14	1.70	0.95 ± 0.30	M	0.52	93	98	37		**63**	
P15	1.78	1.25 ± 0.12	F	0.66	92	100	15		**85**	
P17	1.73	1.23 ± 0.27	F	0.41	83	98			**93**	7
P18	1.74	1.24 ± 0.20	M	0.54	97	100			**97**	3
				Cluster S4: double-step						
P2	1.73	1.04 ± 0.18	M	0.64	96	100	13			**87**
P11	1.84	1.73 ± 0.32	M	0.33	87	93			14	**86**
P13	1.84	1.84 ± 0.26	M	0.50	96	96	4		5	**91**

Relevant demographic information (height and gender) of participants in *session 1* is summarized, together with average (±SD) throw duration and summary results from analysis of the throwing kinematics. This includes the stability index, the recognition rate of the participant's identify obtained using a 5 (5D)- and 10-dimensional 10D) spatiotemporal principal components analysis description of the kinematics, and the percentage of throws assigned to the 4 throwing styles as resulting from cluster analysis. Bold type highlights the most frequent throwing style of each participant. F, female; M, male; S1–S4, *styles 1–4* (NS, no step; RS, right step LS, left step; and DS, double step, respectively).

Representation of individual throwing actions by stPCA coefficients. It is of interest to inspect how different throwers are represented in the stPCA coefficient space. In particular, our first goal was to assess to what extent different throwers are represented in specific subregions of the stPCA coefficient space and if these tend to overlap and/or to cluster into groups. Analogously, it is of interest to explore whether gender is reflected in a preferred subregion.

Figure 4*A* shows (from two different perspectives) the distributions of the stPCA coefficients describing throws from individual participants, represented as covariance ellipsoids in the subspace defined by the first three $\boldsymbol{p}^{ST}$ vectors. The ellipsoid's center corresponds to the coefficients of the individual throwing strategies, namely, the mean across all trials from each participant. The principal semi-axes correspond to the 75% (for better legibility) of the standard deviations in the three directions of higher variability. Individual ellipsoids have a considerable degree of segregation, which increases in subspaces defined by higher order $\boldsymbol{p}^{ST}$ (Supplemental Fig. S5). Furthermore, a trend for clustering of individual ellipsoids in subgroups can be qualitatively appreciated: the region of positive $\boldsymbol{p}_3^{ST}$ coefficients hosts two isolated groups of participants, one group in the subregion of positive $\boldsymbol{p}_1^{ST}$ coefficients (i.e., P6, P10, P19; as visible in Fig. 4*A*, *view 1*) and the other one in the region where $\boldsymbol{p}_1^{ST}$ and $\boldsymbol{p}_2^{ST}$ coefficients are both negative (i.e., P2, P11, P13; as visible in *view 2*).

Similarly, Fig. 4*B* shows the distributions of throws performed by female and male participants, now with ellipsoid semi-axes corresponding to 1 SD. A high degree of separation between the two groups is visible. Female throwers preferentially occupy the region of positive $\boldsymbol{p}_1^{ST}$ and $\boldsymbol{p}_2^{ST}$ coefficients (right step and farther forward projection), whereas males occupy the region of negative coefficients (left step and limited forward projection). Despite the qualitative and intuitive insights offered by these three-dimensional representations, it is not possible to provide a comprehensive visualization of the more complex structures present in stPCA subspaces at higher dimensionalities. The results from analysis techniques tailored for exploring such structures, linear discriminant analysis (LDA) and cluster analysis, are reported below.

Compact stPCA Descriptions of Throwing Actions Allows for Identity and Gender Recognition

Figure 5 shows the results from LDA classification of thrower identity (20-class problem) and gender (2-class problem), as a function of the number of $\boldsymbol{p}^{ST}$ vectors used for reconstructing the kinematics. Figure 5, *A* and *C*, shows the misclassification error (ME). Figure 5, *B* and *D*, shows the confusion matrixes obtained when LDA was run in the 5- and 10-dimensional stPCA spaces for identity and gender recognition, respectively. Remarkably, for both classification problems, a one-dimensional description of throwing actions (the $\boldsymbol{p}_1^{ST}$coefficients alone) allows for MEs well below chance levels: 67% and 34% for identity and gender recognition, respectively, to be compared with the 95% and 50% corresponding chance levels (1 minus the inverse of the number of classes in the problem). Note that the number of trials in our sample, N_t = 2,136, is high enough for the theoretical chance level to be a reliable reference (Combrisson and Jerbi 2015). In both cases, MEs decrease with the number of $\boldsymbol{p}^{ST}$ defining the

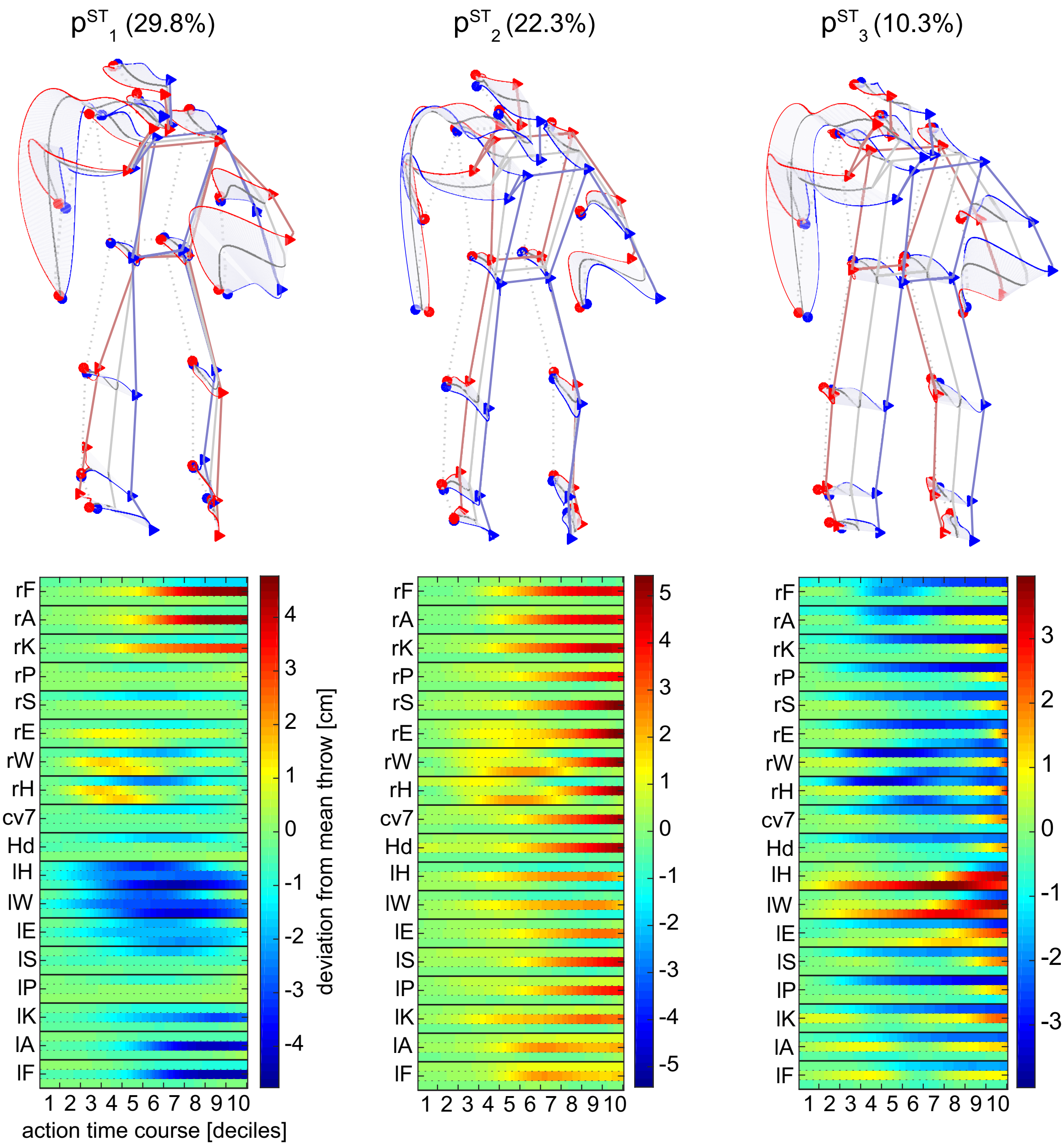

Fig. 3. First three spatiotemporal principal components vectors ($\boldsymbol{p}^{ST}$) represented as mean joint-marker trajectories and as deviation from the mean throw. *Top*: diagrams show how each $\boldsymbol{p}^{ST}$ modulates the joint marker trajectories of the mean throwing kinematics (gray trajectories) when added to (red trajectories) or subtracted from (blue trajectories) the latter with a unitary weight. *Bottom*: heatmaps offer an alternative view of the $\boldsymbol{p}^{ST}$ spatiotemporal structure, showing the displacement from the mean throw (measured in cm) associated to a positive unitary weighted $\boldsymbol{p}^{ST}$ contribution, for the 3 spatial coordinates ([*x*, *y*, *z*] from *top* to *bottom*) of each joint marker and throughout the time course of the action. cv7, Cervical vertebra 7; Hd, head; lA, left ankle; lE, left elbow; lF, left foot; lH, left hand; lK, left knee; lP, left pelvis; lS, left shoulder; lW, left wrist; rA, right ankle; rE, right elbow; rF, right foot; rH, right hand; rK, right knee; rP, right pelvis; rS, right shoulder; rW, right wrist.

predictor space: thus the 10-dimensional description reaches the 2% and 5% ME level for identity and gender recognition, respectively.

Confusion matrixes (CMs) in Fig. 5, *B* and *D*, provide more insights into the results. The CM is a $N_c \times N_c$ matrix, with N_c being the number of classes in the problem. Each CM's element x_{ij} represents the percentage of trials belonging to *class i* and classified as an element of *class j*. Perfect classification corresponds to a CM with all zeros off the diagonal and 100% along the diagonal. For gender recognition, both CMs values given in Fig. 5*D* indicate a higher probability to misclassify females as males than vice versa. This could be due to the larger interindividual variability in the male group. For identity recognition, the CMs structure highlights how most of the misclassified trials belong to the two participants with lower stability indexes, P1 and P20. When P1 and P20 are removed, the average ME decreases from 17% to 11% for the 5-dimensional description and from 2.2% to 1.6% for the 10-dimensional one. In the 10-dimensional case, correct identification rates above 90% can be achieved even for the most unstable participants. This confirms that higher order $\boldsymbol{p}^{ST}$ vectors capture information about subtle features of the indi-

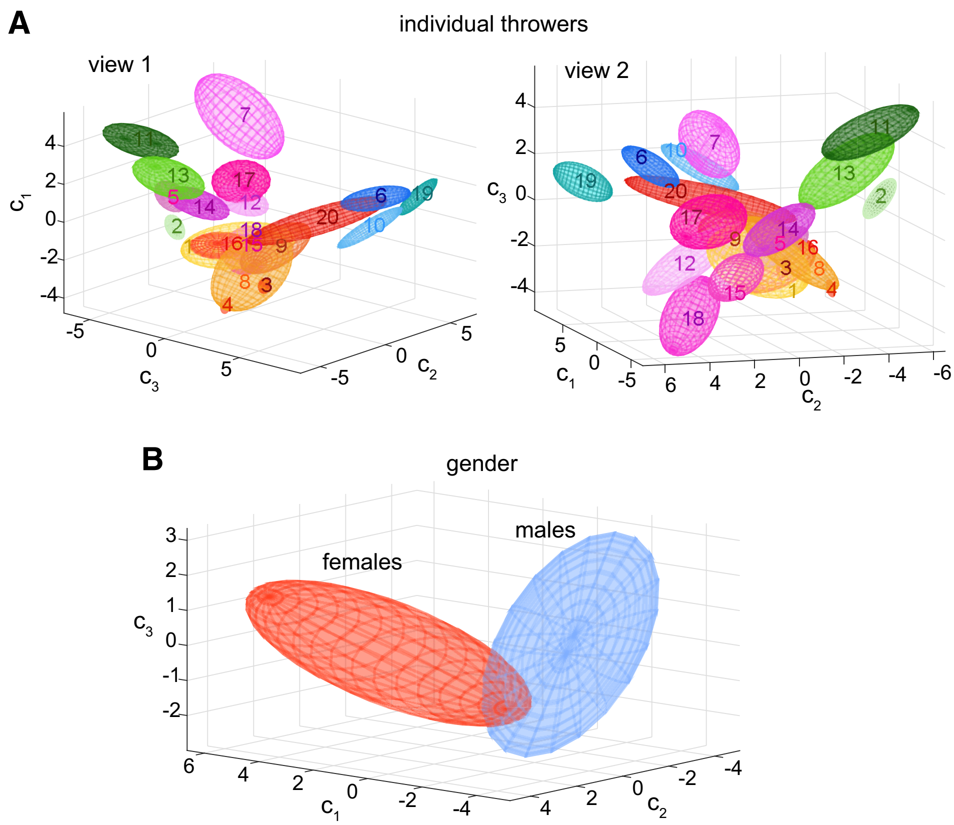

Fig. 4. Individual and gender distributions of throws in the stPCA coefficients space. Distributions are shown in the form of individual covariance ellipsoids in the 3-dimensional subspace defined by the first three $\boldsymbol{p}^{ST}$ vectors. *A*: the center of each ellipsoid corresponds to the coefficients of the mean individual throwing strategy, whereas the principal semi-axes correspond to 0.75 × SD in the 3 directions of higher variability. The ellipsoids are color coded according to the results of the cluster analysis. Bluish and greenish ellipsoids correspond to individuals who have the most trials belonging to right-step and double-step clusters, respectively, whereas yellowish and pinkish ellipsoids correspond to individuals who have the most trials belonging to no-step and left-step clusters, respectively. *View 1* and *view 2* display different visual perspectives of the same 3-dimensional distributions. *B*: distributions of throws performed by female and male participants are shown as ellipsoids centered in the corresponding mean $\boldsymbol{p}^{ST}$ coefficients and with semi-axes corresponding to 1 SD in 3 directions of higher variability.

vidual kinematics, which are missing in the average definition of individual throwing strategies.

Clustering in p^{ST} Coefficient Space Reveals Typical Throwing Styles

We performed cluster analysis with the aim of assessing whether the whole ensemble of throwing actions can be subdivided into a limited number of groups occupying different regions of the stPCA space. Cluster analysis was performed in the five-dimensional stPCA space. LDA showed that this description guarantees high classification accuracy for most participants. We also reasoned that the finer kinematics details captured at higher dimensions should not be relevant when looking for general features of throwing actions shared by multiple individuals.

The Calinski–Harabasz criterion (Calinski and Harabasz 1974), applied to N_k in the range [1,10], indicates that data optimally cluster into $N_k = 4$ groups. This result was confirmed by the Davies–Bouldin (Davies and Bouldin 1979) and the silhouette criteria (Rousseeuw 1987). We additionally tested the hypothesis that our data were structured into clusters, by comparing the normalized Hubert statistics for four clusters with the one obtained for a uniform distribution. Results showed that the null hypothesis that a uniform distribution could explain our data as well as for the case of four clusters can be rejected with a P value <0.01.

Results from the k-means++ method (Arthur and Vassilvitskii 2007) with $N_k = 4$ are shown in Fig. 6. The mean throwing trajectories averaged across all trials assigned to each cluster, independently of the thrower's identity, are shown for the four resulting clusters. We refer to them as typical throwing styles. Each panel of Fig. 6 reports the number of participants with the highest fraction of throws assigned to the corresponding style, their identity, and the fraction of throws assigned to that style for each thrower. For 16 of 20 participants, this fraction is above 85%. The fraction of throws assigned for each participant to the other (nondominant) styles is reported in Table 1. Not surprisingly, P1 and P20, who exhibit the most unstable throwing behavior ($S < 0.31$), are the participants with the lower levels of association with a single style, 33% and 54%, respectively. For P14 and P16, the highest fraction of throws assigned to the same style is instead 63% and 74%, respectively. *Style 1* and *style 3* are the most frequently adopted strategies, whereas *style 2* and *style 4* are adopted less frequently and appear to be gender specific.

To gain more insights on the main features and relative differences characterizing throwing strategies in the four clusters, we quantified differences between pairs of cluster centroids in terms of the distance of the corresponding joint-marker trajectories averaged throughout the action course. The results are plotted in Fig. 7. For all centroid pairs (with the exception of *style 4* vs. *style 3*), the most distant trajectories are associated with the lower limbs. In some cases, and to a lower extent, differences emerge between the trajectories of the throwing arm (*style 2* vs. *style 1*, *style 3* vs. *style 2*, *style 4* vs. *style 2*) and of the left arm (*style 3* vs. *style 1*, *style 3* vs. *style 2*, *style 4* vs. *style 2*). Different is the case of *style 4* vs. *style 3*, for which differences in the average throwing trajectories are milder but distributed throughout the whole body. More details about the spatiotemporal differences across clusters centroids are presented in the Supplemental Fig. S6.

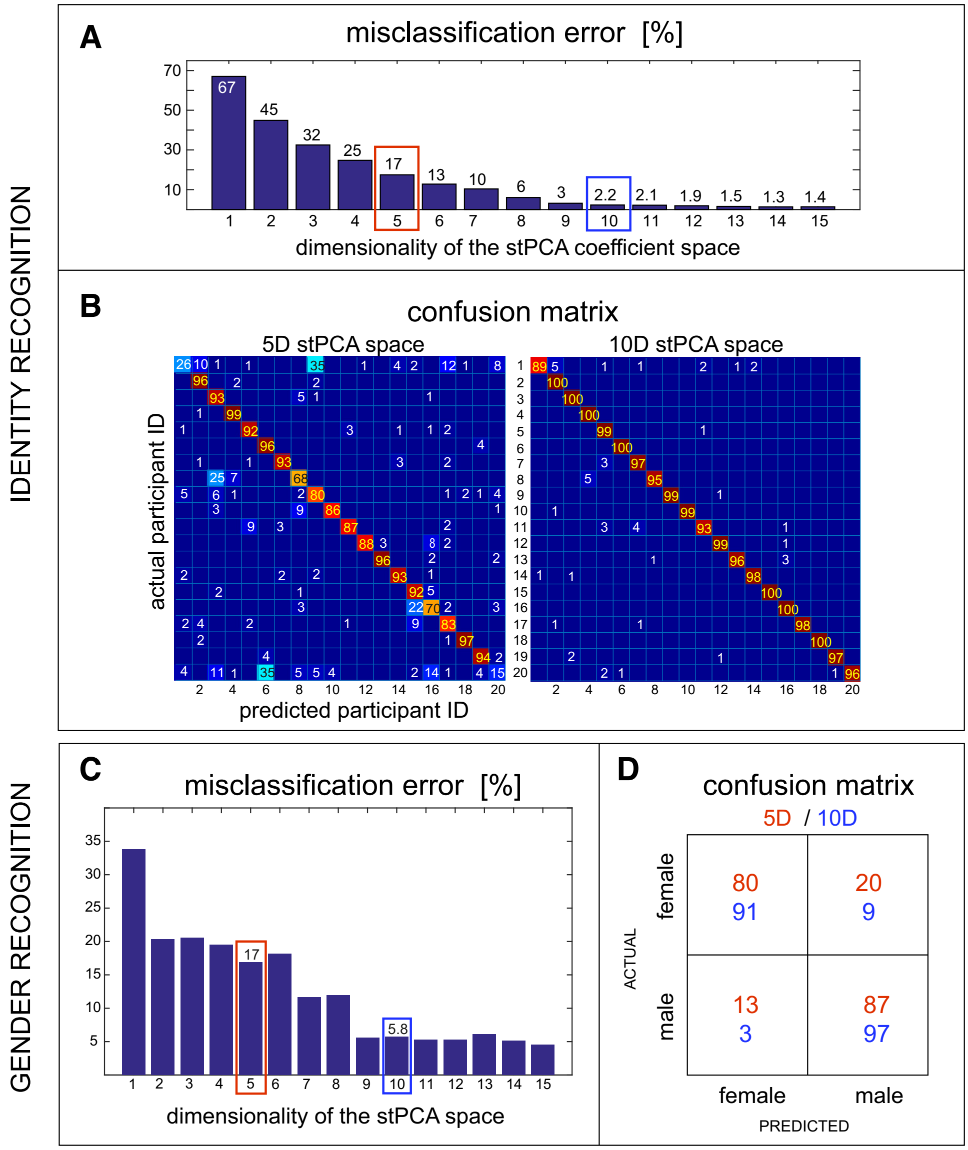

Fig. 5. Results from the linear discriminant analysis for identity and gender recognition. *A* and *C*: the misclassification error, representing the fraction of trials that are misclassified, is shown as a function of the dimensionality of the spatiotemporal principal components analysis (stPCA) subspace adopted as predictor space for identity (*A*) and gender recognition (*C*). *B* and *D*: the confusion matrix (CM) is shown for the two cases in which the 5- and 10-dimensional stPCA subspaces are taken as predictor space for identity (*B*) and gender recognition (*D*). Each CM's element, $x_{ij,}$ represents the percentage of trials belonging to *class i* (row) that are classified as belonging to *class j* (column).

Overall, differences across clusters' centroids point to the stepping pattern as the most prominent source of differentiation between throwing styles. To corroborate that throwing styles correspond to different stepping patterns, we computed the distributions of trials assigned to each cluster in the plane defined by the lengths of the paths traveled by the left and right feet. The results are show in Fig. 8. Trials assigned to *style 1* are concentrated in the vicinity of the origin, corresponding to the large majority of throws performed from a standing posture with no stepping. We indicate this as the no-stepping style. Trials in *style 2* are compressed along the axis of right foot path length L_{RF}, with $L_{\mathrm{LF}} < 10$ cm and peaking at zero, in a region with $L_{\mathrm{RF}} > 40$ cm. We therefore indicate this as the right-step style. *Style 3* was instead designated the left-step style, because its distribution concentrated along the L_{LF} axis, in a region with $L_{\mathrm{LF}} > 40$ cm and values of L_{RF} peaking at zero. Trials in *style 4* occupy preferentially the central part of the plane, i.e., both L_{LF} and L_{RF} are distributed in a region within 20 and 60 cm, corresponding to a double-step pattern. *Style 4* is therefore designated as the double-step style. Whereas the no-step and right-step distributions are very compact and fairly segregated, the left-step and double-step distributions have larger tails that extend toward each other.

We next inspected differences in the throwing arm trajectories associated with different throwing styles. Figure 9 illustrates the right-hand kinematics in the four styles. The solid lines in Fig. 9*A* show the average displacement of the right hand from its initial positions for each style; the corresponding dispersion (time-dependent standard deviation across all trials assigned to each cluster) is shown as shaded area. The wide overlap of the shaded areas indicates that the throwing arm trajectories span the kinematic space in a continuous fashion rather than clustering into discrete groups, as confirmed by cluster analysis performed on the arm kinematics alone (see Supplemental Material). Still, there are interesting differences to highlight. The average trajectory associated with the right-step style clearly deviates from the others, with the preparatory rising phase of the throwing arm preferentially performed by moving the hand forward toward the direction of throw (positive *y*-values) and inward toward the body midline (negative *x*-values). Differences among the remaining three styles are also noticeable: the double-step style is characterized by a later

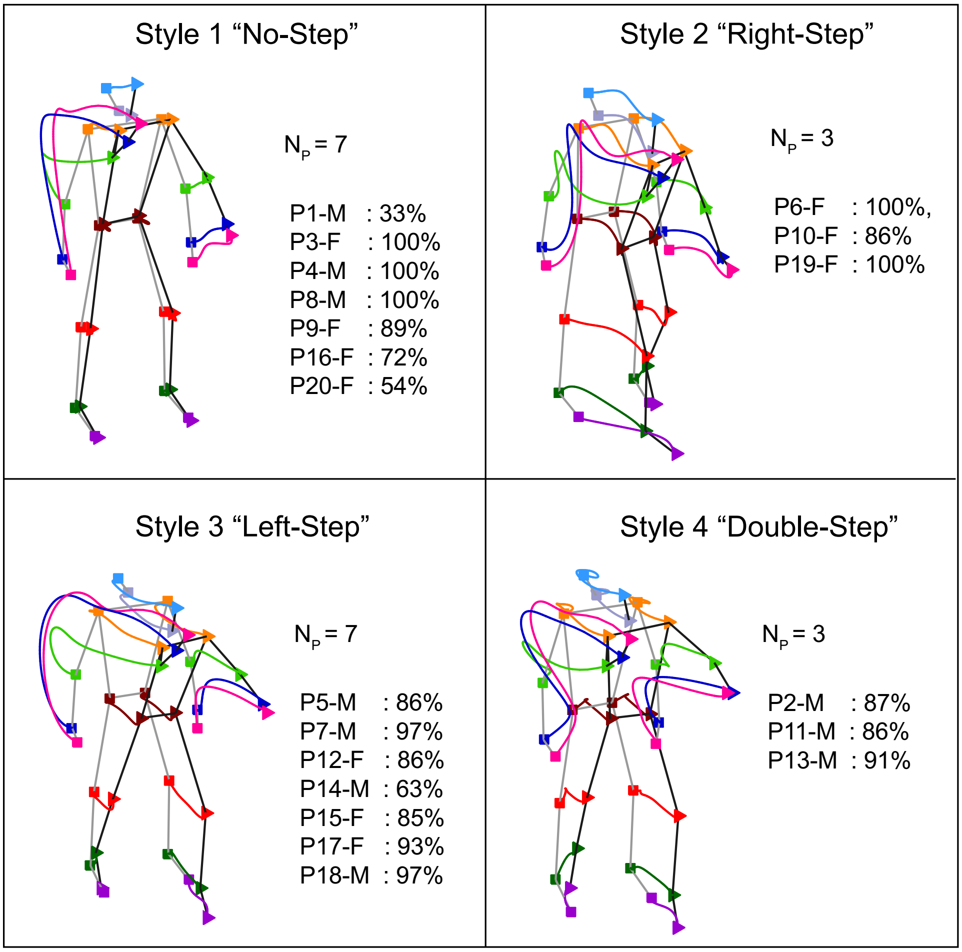

Fig. 6. The four typical throwing styles emerging from cluster analysis. Each panel shows the mean throwing trajectories averaged across all trials assigned to the corresponding cluster, independently of the individual thrower. Different colors correspond to different joint markers. Throwing styles can be adopted by different throwers. Each panel further reports the number of participants for whom the highest fraction of throws is assigned to the corresponding style (N_P), the participant identity (ID; P1–P20), and the fraction of throws that is assigned to the specific throwing style represented. F, female; M, male.

peak of lateral displacement; the left-step style has a prominent early peak in the anterior displacement; and the no-step has a later peak in both lateral and anterior displacement.

To further examine how the throwing arm kinematics vary within each throwing style, we looked at the distribution among throws of lateral and anterior excursions during the rising phase associated with the different throwing styles. Analogously to what done for inspecting the stepping pattern (see Fig. 8), Fig. 9*B* shows the throws counts distribution as a function of the lateral and anterior excursions for all styles. Although, as expected, the distributions are spread, clear peaks are observed that point to the preferred style-specific arm strategy. For the no-step style, the largest peak corresponds to the rising phase of the throwing arm in which the arm opens outward and is kept back, at the level of the shoulders (back-swinging). In the right-step style, most of throws are performed by raising the throwing hand, moving it forward and toward the body midline. The left-step style exhibits instead a marked preference for a back-swinging action of the throwing hand. Finally, in the double-step style, whereas the largest peak corresponds to a back-swinging strategy, a second peak is observed in the region where the throwing hand moves inward. For a closer inspection, trials in the latter peak are all associated with P13, who displays a unique throwing strategy among our sample of 20 participants, consisting in bringing the two hands close together and to the chest before performing a back-swinging action with the throwing arm.

Instability in Individual Throwing Styles Drives Identity Misclassification

We inspected the relationship between instabilities in individual throwing styles and the failing of identity recognition in the five-dimensional description of the throwing kinematics. Both instability and recognition failure are maximum for P1 and P20, who tended to switch between different throwing styles across trials (Table 1), with a seemingly exploratory behavior. Identity-recognition accuracy is also below average (70%) for P16, who also showed occasional changes in throwing techniques from the most recurrent style, the no-step style, to the second choice, the left-step style. In fact, incorrect assignments of P16 throws are attributed mostly to P15, who consistently adopted the left-step styles.

The cases of P14 and P8 are different. Whereas the case of P14 is characterized by a large instability in the throwing style adopted but a high identity-recognition rate, the opposite is true for P8. The latter, who regularly threw with a no-step style, is misclassified with either P3 or P4, both of whom adopted the same style. In this case, misclassification is due to P8's throws being represented in a region of the stPCA space that encompasses those representing both P3's and P4's throws (Fig. 4). On the other hand, although P14 tended to switch from the left-step to the no-step style, the fact that his throws were represented in exclusive ranges of the $\boldsymbol{p}_4^{ST}$ and $\boldsymbol{p}_5^{ST}$ coefficients (Supplemental Fig. S5) ensured an optimal identity recogni-

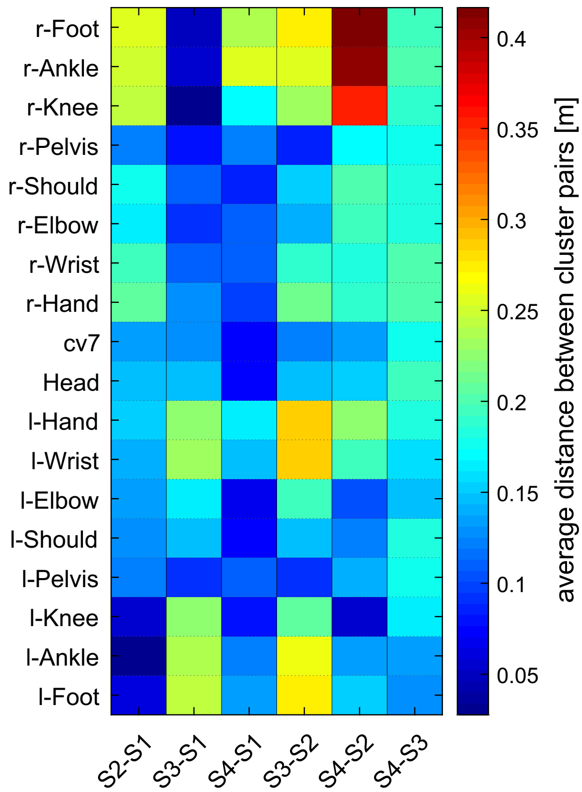

Fig. 7. Kinematics difference between throwing style pairs in body space. Heatmap shows average distance (in meters) between joint markers (*y*-axis) for pairs of throwing trajectories ("styles" S1–S4) associated with the 4 cluster centroids (*x*-axis). Each value mapped is estimated as the distance, averaged over time, of the 2 centroid trajectories associated to a given joint marker. S1, no-step style; S2, right-step style; S3, left-step style; S4, double-step style.

tion. For the same reason, P11 and P12, both represented in a sparsely populated region of the stPCA space (Fig. 4 and Supplemental Fig. S5), are characterized by high identity-recognition rates despite having low stability indexes ($S < 0.36$).

Gender Is Reflected in Different Throwing Styles

As noticed above, the right-step and double-step styles appear to be gender specific, each being populated mainly by females (92% of all right-step throws) and males (98% of all double-step throws), respectively. However, considering the limited number of throwers assigned to these styles ($N = 3$ in each), the gender specificity of these two throwing strategies cannot be generalized. The different combinations of arm trajectories and stepping patterns shown in Figs. 8 and 9 offer additional hints with respect to gender differences. In the no-step group, the throwing arm trajectory differs from the more frequent back-swinging trajectory for all the three female throwers in the group, characterized by throwing arm trajectories in the anterior sagittal plane, similar to those of the throwers of the right-step group (Supplemental Fig. S7). Concordantly, in the left-step group, the only participant displaying this type of throwing arm trajectory was female.

Individual Throwing Styles Tend to Be Stable over Time

We assessed the individual stability in the preferred throwing strategy over time by performing a second recording session (*session 2*) in which we re-recruited six of the *session 1* participants after 22/23 mo (P4, P5, P8, P13, P16, and P20). The new data set was projected onto the $\boldsymbol{p}^{ST}$ vectors extracted from *session 1* so that the new throws could be represented in the stPCA space previously defined. We next used the five-dimensional description to assign new throws to one of the four identified throwing styles, based on minimum distance in the stPCA space. Results are summarized in Fig. 10 and Table 2. Remarkably, after about 2 yr, five of six participants retained their preferred throwing style, which in some cases (P5, P13, and P20) became even more frequent. It is worth noting that the one participant who changed her preferred throwing style (P16) stabilized on her earlier "second choice."

DISCUSSION

The main goal of the current study was to perform quantitative and objective comparisons of overarm throwing behavior within and between individuals. Because we were interested in overarm throwing as a fundamental whole body motor behavior, the study was performed on a sample of untrained adults. By applying a spatiotemporal decomposition to the whole body kinematics of throwing actions, we achieved a very compact yet meaningful representations of complex actions. A five-dimensional stPCA representation of single throws accounted for more than 75% of the total variation observed in more than 2,000 throws from 20 individuals. A 10-dimensional description achieved a 90% level of accuracy. Such extremely compact representations provided features that could be processed by machine learning algorithms to quantitatively characterize and compare individual throwing strategies. We could then relate the throwing kinematics of a specific action to the gender and identity of the thrower with a high degree of accuracy. Moreover, we identified four main throwing styles, mainly differing in the stepping patterns and associated with preferred throwing arm kinematics modes, which are recurrent across individuals. In the following, we discuss how our approach relates to previous methods developed for studying the kinematics of complex whole body movements. We then elaborate on how our results relate to previous literature on the acquisition of throwing skills throughout development, on the marked gender differences observed in throwing proficiencies, and on how complex tasks involving many degrees of freedom can be accomplished with different solutions.

The combination of dimensionality reduction and machine learning techniques is not new in the field of motor behavior. It has been adopted for the analysis of simple reaching tasks (Ansuini et al. 2016), for the analysis of whole body kinematics both in the field of human-computer interaction (Venture et al. 2016; Zhang and Venture 2012) and in the fields of biomechanics and sport science (Huys et al. 2008). The main novelty of our approach consists in the use of the spatiotemporal PCA decomposition for representing the whole body kinematics of complex motor tasks, which are shown to support remarkably compact representations of the complex kinematics characterizing noncyclic actions. Conventional PCA, largely used for the representation of whole body movements (Daffertshofer et al. 2004; Gløersen et al. 2018; Huys et al. 2008), implies the identification of principal postures that are linearly combined with time-dependent weight coefficients. By adopting a stPCA decomposition, it is instead possible to represent complex

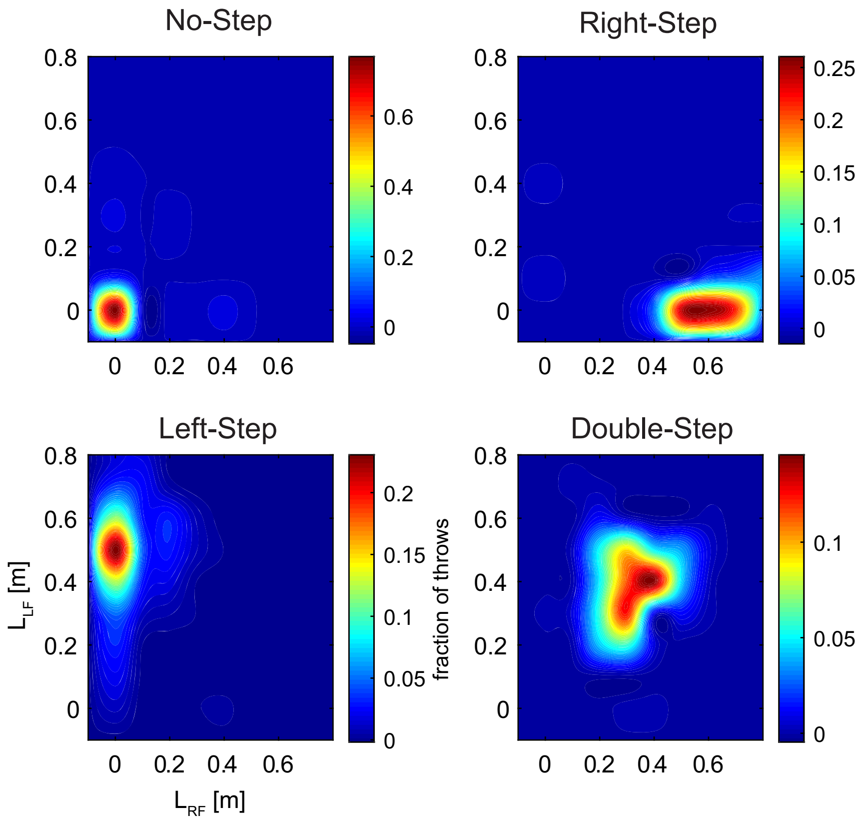

Fig. 8. Normalized and smoothed distributions of throws counts are shown for the 4 throwing styles as a function of the path lengths of the right (L_{RF}) and left foot (L_{LF}).

actions as linear combinations of principal "movements" weighted by scalar coefficients, which makes the resulting representation more compact (see Russo et al. 2014 for a formal comparison of the two methods). The difference is particularly relevant for the representation of noncyclic actions that, differently from the case of cyclic type of motor behavior (e.g., walking, running, and skiing), do not support the extraction of few parameters (e.g., period or amplitude) from the time-dependent PCA coefficients. At the same time, stPCA is characterized by the same limitations of standard PCA as a means to represent biological motion (Federolf et al., 2014). One of the most relevant limitation is the fact that the resulting vector space is defined in terms of principal vectors that do not automatically provide information about control strategies and biomechanical functions. Furthermore, the specific shape of PC vectors depends on the reference frame in which the kinematics are originally described and on the specific data set used for the extraction. This implies that the shape of the principal vectors will not always guarantee optimal performances in terms of dimensionality reduction, nor always guarantee to disentangle movement components that may be truly dissociable in terms of control strategy. Here, however, we do not adopt the stPCA representation as an end-point description of the kinematics, but as a tool supporting an unbiased quantitative comparison of throwing actions across and within individuals. For this reason, the limitations discussed above play a minor role on the outcomes of our study, which highlight the identity and gender footprints entailed in the whole body kinematics of throwing actions and the existence of four main throwing styles recurrent across individuals.

The mean kinematics associated with the four typical throwing styles emerging from cluster analysis present some surprising analogies with the different "stages" of throwing skill acquisition during development. Previous studies have highlighted specific sequences in the acquisition of skilled throwing, in which different motor patterns progressively emerge in the whole body kinematics. The first of these studies distinguished four stages, progressively acquired from about age 2 to 6 yr (Wild 1938). From a stationary base of support, throwing typically evolves into a weight-shifting stepping mode; concurrently, the throwing arm trajectory shifts from an anterior-posterior to a horizontal plane. The first two stages are characterized by a stationary support, with the arm kinematics initially moving in the anterior sagittal plane (years 2 to 3) and then shifting toward a lateral horizontal plane with the involvement of trunk rotation (years 3 to 5). Next, stepping patterns emerge; first with the leg ipsilateral to the throwing arm moving forward (years 5 to 6), and eventually with the contralateral leg. Other authors refined this coarse categorization highlighting different developmental stages in a set of body-part-specific components, focusing in particular on the trunk rotation and the throwing arm movements in the preparatory and forward swing phases (Roberton 1977; Roberton et al. 1979). Different components may proceed throughout their specific skill acquisition sequence at different rates, resulting in a variety of whole body throwing profiles observable within and across throwers (Langendorfer and Roberton 2002; Payne and Isaacs 2012).

Generally, during development, preparatory movements are progressively introduced in the throwing behavior that tends to eventually converge toward a profile that optimizes forceful throws and is indeed evident in fast-ball sports athletes (Stodden et al. 2006a, 2006b). However, not all individuals achieve this final stage, because skill acquisition can stop progressing

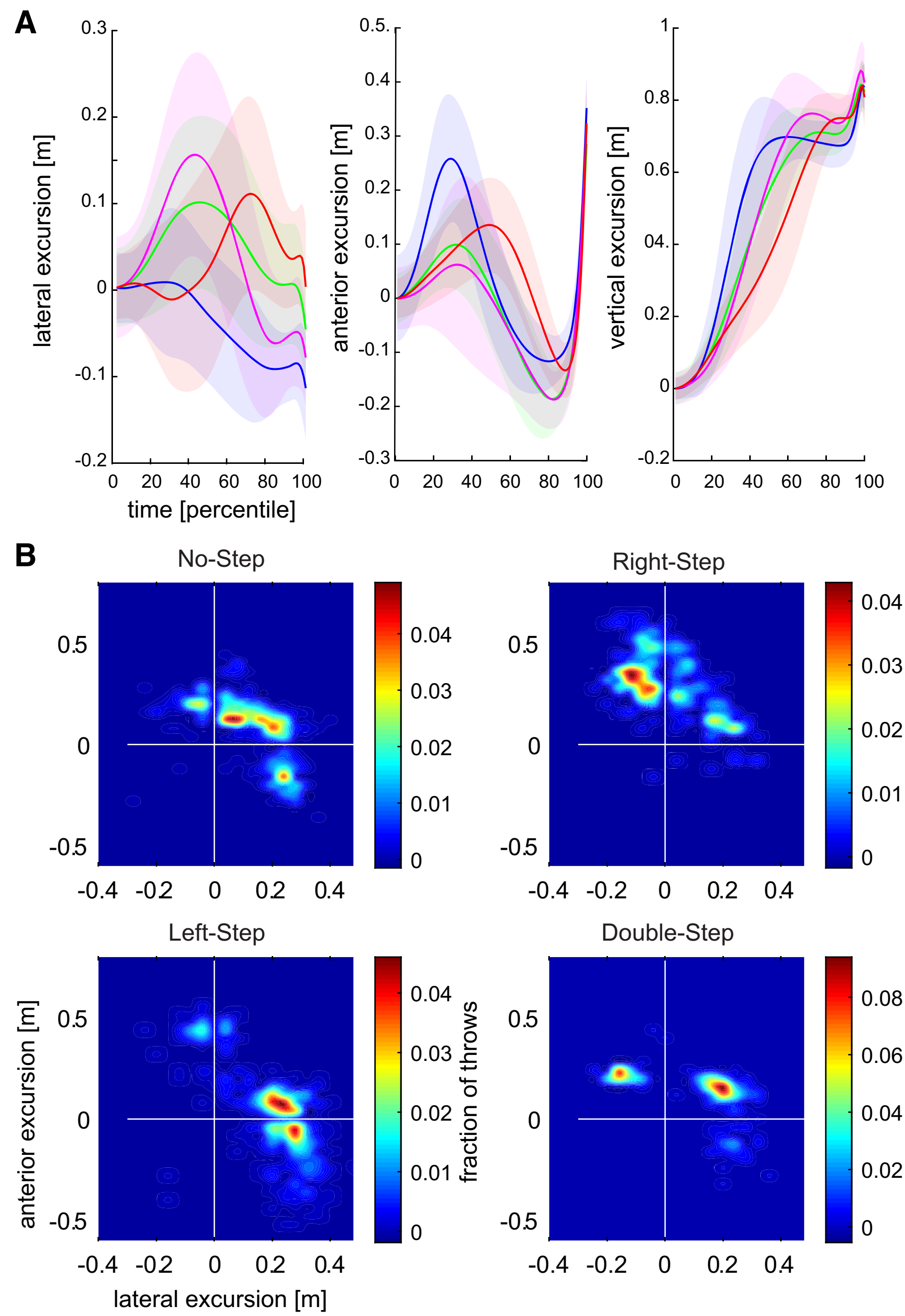

Fig. 9. Throwing (right)-hand kinematics in the 4 whole body throwing styles. *A*: mean (averaged across trials assigned to each cluster) lateral (*left*), anterior (*middle*), and vertical (*right*) excursions (displacement from the initial position) of the hand as a function of the time throughout the action course, from action onset to ball release. The shown kinematics is described in the body reference frame, with the *x-z* plane aligned with the frontal plane and the *y*-axis pointing in the direction of throw. Solid curves correspond to the 4 cluster centroids (i.e., the kinematics averaged across all throws assigned to each cluster): green, no-step cluster; blue, right-step cluster; magenta, left -step cluster; and red, double-step cluster. Shaded areas show the corresponding (same color coding) SD. *B*: normalized and smoothed distributions of throw counts are shown for the 4 throwing styles as a function of the lateral and anterior excursions of the throwing hand during the rising phase of the throwing action.

at a certain stage of development. A clear gender gap in throwing proficiency is retained throughout development, and girls are more prone to stabilize at an intermediate stage of throwing proficiency (Butterfield et al. 2012; Nelson et al. 1991; Petranek and Barton 2011). Unbiased results from our clustering analysis are in line with these general observations. Whereas the four typical styles emerging from the cluster analysis nearly correspond to the main stages in the skill acquisition sequence first reported by Wild (1938), the presence of different throwing arm kinematics within each main style is in line with the component approach of Roberton and colleagues (Langendorfer and Roberton 2002). In fact, a given stage of development in the feet movement components may be combined with different stages in the arm movement components. The gender representation that we found in combinations of components characterizing individual throwing strategies is in agreement with the established evidence that females are typically less proficient than males in overarm throwing throughout development and that they stop earlier on the different possible branches of skill acquisition (Nelson et al. 1991; Young 2009).

The emergence of a limited number of typical throwing styles, recurrent across participants and in most cases stable within participants, has important implications in the context of motor control studies. Previous researchers have discussed how humans, when facing a complex motor task, may adopt multiple solutions (Ganesh and Burdet 2013). This behavior is different from that observed for simple motor tasks, such as a reach-to-grasp action, in which the central nervous system (CNS) tends to select the one solution, among a set of virtually

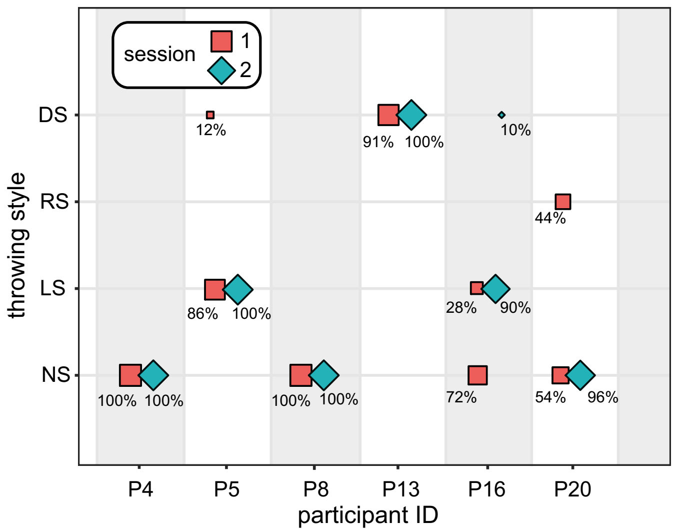

Fig. 10. Stability of throwing styles over time. Symbols represent throwing styles adopted by participants in at least 10% of the throws performed in *session 1* (red squares) and *session 2* (blue diamonds). The two sessions are separated in time by 22/23 mo. For all participants, the actual percentage of throws assigned to a given style is reported next to the corresponding symbol, and it is reflected by the size of the symbol. NS, no step; LS, left step; RS, right step; DS, double step. In general, individual preferred throwing styles are retained, and in some cases stabilize, over time. Only participant P16 changed her preferred throwing style in *session 2* to what had been her "second choice" in *session 1*.

infinite possibilities, that simultaneously minimizes the metabolic cost of the action and the error (Burdet and Milner 1998; Harris and Wolpert 1998). In complex tasks, instead, motor behavior is not driven by global optimization, since distant local minima exist corresponding to different motor plans that solve the task in suboptimal manners (Ganesh and Burdet 2013; Kodl et al. 2011). The selection of a specific solution may emerge from the interaction between motor memories and local minimization of error and effort (Ganesh et al. 2010). In particular, while learning complex motor tasks, humans often adopt exploratory behavior, which serves for gathering information about the landscape of the possible solutions and about the tolerance of such solutions to the motor variability intrinsic to the CNS (Cusumano and Cesari 2006; Müller and Sternad 2009). With practice, explorative behaviors tend to dampen as the task execution converges toward a single solution, not necessarily the optimal one (Ganesh et al. 2010; Müller and Sternad 2004). In this framework, the typical throwing styles we found, and their substyles observable at the level of individual strategies, may be regarded as possible counterparts of local minima of a cost-function manifold. The finding that most participants were stable in their throwing strategy suggests that, in adulthood, throwing is typically an acquired motor plan that does not recruit explorative strategies. Results from the second session confirm this conclusion. All the retested participants exhibiting a stable throwing behavior during the first session retained their style even after 2 yr. The throwers who were instead unstable, showing a more exploratory behavior in the first session, tended to stabilize with time into one of the preferred solutions previously adopted. Because of the small sample size of *session 2*, however, these considerations should be regarded as tentative conclusions and will require further confirmation.

The combination of stPCA representations with linear discriminant and cluster analyses presented in this study provides an innovative method for studying the whole body kinematics of naturalistic motor behaviors. In the context of overarm throwing, the results presented here serve as a first step in this direction and could be further extended to address more in depth some of the important aspects that developmental and gender studies have raised in the past. For example, our cluster analysis does not capture the multilevel structure of the "components" approach, in which the kinematics of the different body parts can be combined at different developmental stages, resulting in a branching structure of possible individual throwing techniques (Langendorfer and Roberton 2002). This may be due to different stepping patterns being well segregated in the stPCA representation, whereas the kinematics of the throwing arm span, within and across participants, a more continuous region of the stPCA coefficient space. A higher dimensional description of the kinematics, combined with a hierarchical clustering approach, may possibly capture such branching structures. However, this goes beyond the scope of the present study. Similarly, the mechanisms governing the way in which the unstable behavior observed in some throwers evolves both across trials within a single session, and across sessions spaced in time, deserve further investigation.

The approach proposed here for the study of throwing behavior can be adopted for a large variety of naturalistic motor actions and real-life motor skills, from sporting performances to daily living activities. In turn, this could pave the way for a variety of quantitative studies aimed at characterizing interindividual and intraindividual variability in complex naturalistic motor behaviors, with a spectrum of possible applications that range from medical diagnosis to autonomous recog-

Table 2. *Percentage of throws assigned to four throwing styles previously identified based on session 1*

	Style Assigned							
	No Step		Right Step		Left Step		Double Step	
Participant ID	*Session 1*	*Session 2*	*Session 1*	*Session 2*	*Session 1*	*Session 2*	*Session 1*	*Session 2*
P4	**100**	**100**						
P5	2				**86**	**100**	12	
P8	**100**	**100**						
P13	4				5		**91**	**100**
P16	**72**				28	**90**		10
P20	**54**	**96**	44	2	2			

Values are, for both *session 1* and *session 2*, the percentages of throws assigned to the 4 throwing styles as resulting from cluster analysis. Bold type highlights the most frequent throwing style of individual participants for both experimental sessions.

nition of identity and/or activities in human computer interaction.

ACKNOWLEDGMENTS

We thank Paolo Tommasino for helping with data collection in *session 2*, and Etienne Burdet for reading and providing suggestions on the final version of the manuscript.

Present addresses: A. Dhawan, EDGE10(UK) Ltd. 10D Printing House Yard, Hackney Road, London, UK E2 7PR; M. Russo, Dept. of Biology, Northeastern University, Boston, MA 02115.

GRANTS

This work was supported by Horizon 2020 Robotics Program CogIMon (ICT-23-2014 under Grant Agreement 644727), the Italian Ministry of Health (IRCCS Ricerca corrente), the Italian Education, University and Research Ministry (PRIN Grants 2015HFWRYY and 2017CBF8NJ_005), and the Italian Space Agency (Contracts No. I/006/06/0 and 2019-11-U.0).

DISCLOSURES

No conflicts of interest, financial or otherwise, are declared by the author(s).

AUTHOR CONTRIBUTIONS

A.M., A.D., F.L., and A.dA. conceived and designed research; A.M., A.D., M.R., and B.C. performed experiments; A.M. analyzed data; A.M. interpreted results of experiments; A.M. prepared figures; A.M. drafted manuscript; A.M., A.D., M.R., F.L., and A.dA. edited and revised manuscript; A.M., A.D., M.R., B.C., F.L., and A.dA. approved final version of manuscript.

REFERENCES

Ansuini C, Cavallo A, Campus C, Quarona D, Koul A, Becchio C. Are we real when we fake? Attunement to object weight in natural and pantomimed grasping movements. *Front Hum Neurosci* 10: 471, 2016. doi:10.3389/fnhum.2016.00471.

Arthur D, Vassilvitskii S. K-means++: the advantages of careful seeding. In: *Proceedings of the Eighteenth Annual ACM-SIAM Symposium on Discrete Algorithms*, edited by Gabow H. Philadelphia, PA: Society for Industrial and Applied Mathematics, 2007, vol. 8, p. 1027–1025.

Bartlett R, Wheat J, Robins M. Is movement variability important for sports biomechanists? *Sports Biomech* 6: 224–243, 2007. doi:10.1080/14763140701322994.

Bernstein NA. *The Co-ordination and Regulation of Movements*. Oxford, UK: Pergamon, 1967.

Burdet E, Milner TE. Quantization of human motions and learning of accurate movements. *Biol Cybern* 78: 307–318, 1998. doi:10.1007/s004220050435.

Butterfield SA, Angell RM, Mason CA. Age and sex differences in object control skills by children ages 5 to 14. *Percept Mot Skills* 114: 261–274, 2012. doi:10.2466/10.11.25.PMS.114.1.261-274.

Butterfield SA, Loovis EM. Influence of age, sex, balance, and sport participation on development of throwing by children in grades K–8. *Percept Mot Skills* 76: 459–464, 1993. doi:10.2466/pms.1993.76.2.459.

Calinski T, Harabasz J. A dendrite method for cluster analysis. *Commun Stat Theory Methods* 3: 1–27, 1974. doi:10.1080/03610927408827101.

Calvin WH. Did throwing stones shape hominid brain evolution? *Ethol Sociobiol* 3: 115–124, 1982. doi:10.1016/0162-3095(82)90010-3.

Calvin WH. A stone's throw and its launch window: timing precision and its implications for language and hominid brains. *J Theor Biol* 104: 121–135, 1983. doi:10.1016/0022-5193(83)90405-8.

Cesqui B, d'Avella A, Portone A, Lacquaniti F. Catching a ball at the right time and place: individual factors matter. *PLoS One* 7: e31770, 2012. doi:10.1371/journal.pone.0031770.

Clever D, Malin Schemschat R, Felis ML, Mombaur K. Inverse optimal control based identification of optimality criteria in whole-body human walking on level ground. *2016 6th IEEE International Conference on Biomedical Robotics and Biomechatronics (BioRob)*. 2016: 1192–1199, 2016. doi:10.1109/BIOROB.2016.7523793

Combrisson E, Jerbi K. Exceeding chance level by chance: the caveat of theoretical chance levels in brain signal classification and statistical assessment of decoding accuracy. *J Neurosci Methods* 250: 126–136, 2015. doi:10.1016/j.jneumeth.2015.01.010.

Cusumano JP, Cesari P. Body-goal variability mapping in an aiming task. *Biol Cybern* 94: 367–379, 2006. doi:10.1007/s00422-006-0052-1.

Daffertshofer A, Lamoth CJ, Meijer OG, Beek PJ. PCA in studying coordination and variability: a tutorial. *Clin Biomech (Bristol, Avon)* 19: 415–428, 2004. doi:10.1016/j.clinbiomech.2004.01.005.

Darlington PJ Jr. Group selection, altruism, reinforcement, and throwing in human evolution. *Proc Natl Acad Sci USA* 72: 3748–3752, 1975. doi:10.1073/pnas.72.9.3748.

Darwin C. *The Descent of Man, and Selection in Relation to Sex*. London, UK: John Murray, 1871.

Davies DL, Bouldin DW. A cluster separation measure. *IEEE Trans Pattern Anal Mach Intell* 1: 224–227, 1979. doi:10.1109/TPAMI.1979.4766909.

Escamilla RF, Andrews JR. Shoulder muscle recruitment patterns and related biomechanics during upper extremity sports. *Sports Med* 39: 569–590, 2009. doi:10.2165/00007256-200939070-00004.

Federolf P, Reid R, Gilgien M, Haugen P, Smith G. The application of principal component analysis to quantify technique in sports. *Scand J Med Sci Sports* 24: 491–499, 2014. doi:10.1111/j.1600-0838.2012.01455.x.

Flash T, Hogan N. The coordination of arm movements: an experimentally confirmed mathematical model. *J Neurosci* 5: 1688–1703, 1985. doi:10.1523/JNEUROSCI.05-07-01688.1985.

Fleisig GS, Andrews JR, Dillman CJ, Escamilla RF. Kinetics of baseball pitching with implications about injury mechanisms. *Am J Sports Med* 23: 233–239, 1995. doi:10.1177/036354659502300218.

Fleisig GS, Barrentine SW, Zheng N, Escamilla RF, Andrews JR. Kinematic and kinetic comparison of baseball pitching among various levels of development. *J Biomech* 32: 1371–1375, 1999. doi:10.1016/S0021-9290(99)00127-X.

Ganesh G, Burdet E. Motor planning explains human behaviour in tasks with multiple solutions. *Robot Auton Syst* 61: 362–368, 2013. doi:10.1016/j.robot.2012.09.024.

Ganesh G, Haruno M, Kawato M, Burdet E. Motor memory and local minimization of error and effort, not global optimization, determine motor behavior. *J Neurophysiol* 104: 382–390, 2010. doi:10.1152/jn.01058.2009.

Gløersen Ø, Myklebust H, Hallén J, Federolf P. Technique analysis in elite athletes using principal component analysis. *J Sports Sci* 36: 229–237, 2018. doi:10.1080/02640414.2017.1298826.

Goodall J. Tool-using and aimed throwing in a community of free-living chimpanzees. *Nature* 201: 1264–1266, 1964. doi:10.1038/2011264a0.

Gromeier M, Koester D, Schack T. Gender differences in motor skills of the overarm throw. *Front Psychol* 8: 212, 2017. doi:10.3389/fpsyg.2017.00212.

Harris CM, Wolpert DM. Signal-dependent noise determines motor planning. *Nature* 394: 780–784, 1998. doi:10.1038/29528.

Hirashima M, Yamane K, Nakamura Y, Ohtsuki T. Kinetic chain of overarm throwing in terms of joint rotations revealed by induced acceleration analysis. *J Biomech* 41: 2874–2883, 2008. doi:10.1016/j.jbiomech.2008.06.014.

Hopkins WD, Russell JL, Schaeffer JA. The neural and cognitive correlates of aimed throwing in chimpanzees: a magnetic resonance image and behavioural study on a unique form of social tool use. *Philos Trans R Soc Lond B Biol Sci* 367: 37–47, 2012. doi:10.1098/rstb.2011.0195.

Hore J. Motor control, excitement, and overarm throwing. *Can J Physiol Pharmacol* 74: 385–389, 1996.

Hore J, Watts S. Timing finger opening in overarm throwing based on a spatial representation of hand path. *J Neurophysiol* 93: 3189–3199, 2005. doi:10.1152/jn.01268.2004.

Hore J, Watts S. Skilled throwers use physics to time ball release to the nearest millisecond. *J Neurophysiol* 106: 2024–2033, 2011. doi:10.1152/jn.00059.2011.

Hore J, Watts S, Martin J, Miller B. Timing of finger opening and ball release in fast and accurate overarm throws. *Exp Brain Res* 103: 277–286, 1995. doi:10.1007/BF00231714.

Hore J, Watts S, Tweed D. Errors in the control of joint rotations associated with inaccuracies in overarm throws. *J Neurophysiol* 75: 1013–1025, 1996. doi:10.1152/jn.1996.75.3.1013.

Huys R, Smeeton NJ, Hodges NJ, Beek PJ, Williams AM. On the dynamic information underlying visual anticipation skill. *Percept Psychophys* 70: 1217–1234, 2008. doi:10.3758/PP.70.7.1217.

Klein Breteler MD, Simura KJ, Flanders M. Timing of muscle activation in a hand movement sequence. *Cereb Cortex* 17: 803–815, 2007. doi:10.1093/cercor/bhk033.

Kodl J, Ganesh G, Burdet E. The CNS stochastically selects motor plan utilizing extrinsic and intrinsic representations. *PLoS One* 6: e24229, 2011. doi:10.1371/journal.pone.0024229.

La Scaleia B, Zago M, Lacquaniti F. Hand interception of occluded motion in humans: a test of model-based vs. on-line control. *J Neurophysiol* 114: 1577–1592, 2015. doi:10.1152/jn.00475.2015.

Langendorfer SJ, Roberton MA. Individual pathways in the development of forceful throwing. *Res Q Exerc Sport* 73: 245–256, 2002. doi:10.1080/02701367.2002.10609018.

Lees A. Technique analysis in sports: a critical review. *J Sports Sci* 20: 813–828, 2002. doi:10.1080/026404102320675657.

Lombardo MP, Deaner RO. On the evolution of the sex differences in throwing: throwing is a male adaptation in humans. *Q Rev Biol* 93: 91–119, 2018a. doi:10.1086/698225.

Lombardo MP, Deaner RO. Born to throw: the ecological causes that shaped the evolution of throwing in humans. *Q Rev Biol* 93: 1–16, 2018b. doi:10.1086/696721.

Mardia KV, Kent JT, Bibby JN. *Multivariate Analysis*. San Diego, CA: Academic, 1979.

Maselli A, Dhawan A, Cesqui B, Russo M, Lacquaniti F, d'Avella A. Where are you throwing the ball? I better watch your body, not just your arm! *Front Hum Neurosci* 11: 505, 2017. doi:10.3389/fnhum.2017.00505.

Morasso P. Spatial control of arm movements. *Exp Brain Res* 42: 223–227, 1981. doi:10.1007/BF00236911.

Müller H, Sternad D. Decomposition of variability in the execution of goal-oriented tasks: three components of skill improvement. *J Exp Psychol Hum Percept Perform* 30: 212–233, 2004. doi:10.1037/0096-1523.30.1.212.

Müller H, Sternad D. Motor learning: changes in the structure of variability in a redundant task. *Adv Exp Med Biol* 629: 439–456, 2009. doi:10.1007/978-0-387-77064-2_23.

Nelson KR, Thomas JR, Nelson JK. Longitudinal change in throwing performance: gender differences. *Res Q Exerc Sport* 62: 105–108, 1991. doi:10.1080/02701367.1991.10607526.

Pappas AM, Zawacki RM, Sullivan TJ. Biomechanics of baseball pitching. A preliminary report. *Am J Sports Med* 13: 216–222, 1985. doi:10.1177/036354658501300402.

Pataky TC, Robinson MA, Vanrenterghem J. Vector field statistical analysis of kinematic and force trajectories. *J Biomech* 46: 2394–2401, 2013 [Erratum in *J Biomech* 48: 190–192, 2015]. doi:10.1016/j.jbiomech.2013.07.031.

Payne GV, Isaacs LD. *Human Motor Development: A Lifespan Approach* (8th ed.). New York: McGraw-Hill, 2012.

Petranek LJ, Barton GV. The overarm-throwing pattern among U-14 ASA female softball players: a comparative study of gender, culture, and experience. *Res Q Exerc Sport* 82: 220–228, 2011. doi:10.1080/02701367.2011.10599749.

Roach NT, Lieberman DE. Upper body contributions to power generation during rapid, overhand throwing in humans. *J Exp Biol* 217: 2139–2149, 2014. doi:10.1242/jeb.103275.

Roach NT, Richmond BG. Clavicle length, throwing performance and the reconstruction of the Homo erectus shoulder. *J Hum Evol* 80: 107–113, 2015. doi:10.1016/j.jhevol.2014.09.004.

Roach NT, Venkadesan M, Rainbow MJ, Lieberman DE. Elastic energy storage in the shoulder and the evolution of high-speed throwing in Homo. *Nature* 498: 483–486, 2013. doi:10.1038/nature12267.

Roberton MA. Stability of stage categorizations across trials: implications for the "stage theory" of overarm throw development. *J Hum Mov Stud* 3: 49–59, 1977.

Roberton MA, Halverson LE, Langendorfer S, Williams K. Longitudinal changes in children's overarm throw ball velocities. *Res Q* 50: 256–264, 1979. doi:10.1080/10671315.1979.10615608.

Rousseeuw PJ. Silhouettes: a graphical aid to the interpretation and validation of cluster analysis. *J Comput Appl Math* 20: 53–65, 1987. doi:10.1016/0377-0427(87)90125-7.

Russo M, D'Andola M, Portone A, Lacquaniti F, d'Avella A. Dimensionality of joint torques and muscle patterns for reaching. *Front Comput Neurosci* 8: 24, 2014. doi:10.3389/fncom.2014.00024.

Sachlikidis A, Salter C. A biomechanical comparison of dominant and non-dominant arm throws for speed and accuracy. *Sports Biomech* 6: 334–344, 2007. doi:10.1080/14763140701491294.

Seroyer ST, Nho SJ, Bach BR, Bush-Joseph CA, Nicholson GP, Romeo AA. The kinetic chain in overhand pitching: its potential role for performance enhancement and injury prevention. *Sports Health* 2: 135–146, 2010. doi:10.1177/1941738110362656.

Southard D. Change in throwing pattern: critical values for control parameter of velocity. *Res Q Exerc Sport* 73: 396–407, 2002. doi:10.1080/02701367.2002.10609039.

Southard D. Throwing pattern: changes in timing of joint lag according to age between and within skill level. *Res Q Exerc Sport* 80: 213–222, 2009. doi:10.1080/02701367.2009.10599555.

Stodden DF, Fleisig GS, McLean SP, Andrews JR. Relationship of biomechanical factors to baseball pitching velocity: within pitcher variation. *J Appl Biomech* 21: 44–56, 2005. doi:10.1123/jab.21.1.44.

Stodden DF, Langendorfer SJ, Fleisig GS, Andrews JR. Kinematic constraints associated with the acquisition of overarm throwing part I: step and trunk actions. *Res Q Exerc Sport* 77: 417–427, 2006a. doi:10.1080/02701367.2006.10599377.

Stodden DF, Langendorfer SJ, Fleisig GS, Andrews JR. Kinematic constraints associated with the acquisition of overarm throwing part II: upper extremity actions. *Res Q Exerc Sport* 77: 428–436, 2006b. doi:10.1080/02701367.2006.10599378.

Theodoridis S, Koutroumbas K. *Pattern Recognition*. New York: Academic, 1999.

Thomas JR, French KE. Gender differences across age in motor performance a meta-analysis. *Psychol Bull* 98: 260–282, 1985. doi:10.1037/0033-2909.98.2.260.

Thomas JR, Michael D, Gallagher JD. Effects of training on gender differences in overhand throwing: a brief quantitative literature analysis. *Res Q Exerc Sport* 65: 67–71, 1994. doi:10.1080/02701367.1994.10762209.

Urbin MA. Sensorimotor control in overarm throwing. *Mot Contr* 16: 560–578, 2012. doi:10.1123/mcj.16.4.560.

Urbin MA, Stodden DF, Fleisig GS. Overarm throwing variability as a function of trunk action. *J Mot Learn Dev* 1: 89–95, 2013. doi:10.1123/jmld.1.4.89.

Venture G, Yabuki T, Kinase Y, Berthoz A, Abe N. Using dynamics to recognize human motion. In: *Dance Notations and Robot Motions*, edited by Laumon JP, Abe N. Basel: Springer, 2016, p. 361–371.

Whiteley R. Baseball throwing mechanics as they relate to pathology and performance–a review. *J Sports Sci Med* 6: 1–20, 2007.

Wild MR. The behavior pattern of throwing and some observations concerning its course of development in children. *Res Quarterly Am Assoc Heal Phys Educ* 9: 20–24, 1938. doi:10.1080/23267429.1938.11802445.

Williams HG, Monsma E. Assessment of gross motor development. In: *Psychoeducational Assessment of Preschool Children* (4th ed.), edited by Bracken BA, Nagle RJ. Hillsdale, NJ: Erlbaum, 2006, p. 204–233.

Wilson AD, Zhu Q, Barham L, Stanistreet I, Bingham GP. A dynamical analysis of the suitability of prehistoric spheroids from the cave of hearths as thrown Projectiles. *Sci Rep* 6: 30614, 2016. doi:10.1038/srep30614.

Young RW. The ontogeny of throwing and striking. *Hum Ontogenetics* 3: 19–31, 2009. doi:10.1002/huon.200800013.

Zhang T, Venture G. Individual recognition from gait using feature value method. *Cybern Inf Technol* 12: 86–95, 2012. doi:10.2478/cait-2012-0024.